



Radiation calculations for fireball and jet fire models: A literature review

Prepared by researchers at the
Health and Safety Executive

RR1196 (2023)

Research Report

© Crown copyright 2023

Prepared 2023

First published 2023

You may reuse this information (not including logos) free of charge in any format or medium, under the terms of the Open Government Licence. To view the licence: visit the [National Archives Website](#), write to the Information Policy Team, The National Archives, Kew, London TW9 4DU, or email psi@nationalarchives.gsi.gov.uk.

Some images and illustrations may not be owned by the Crown so cannot be reproduced without permission of the copyright owner. Enquiries should be sent to copyright@hse.gov.uk.

The Health and Safety Executive (HSE) is a statutory consultee for planning applications around major hazard sites and pipelines and on applications for hazardous substances consent. HSE's advice is aimed at mitigating the effects of a major accident on the population around a major hazard site. This advice is informed by the use of mathematical models of potential hazards. HSE has an ongoing research programme to assess the suitability of the models used.

One of the potential hazards considered is a fireball or a jet fire that produces intense thermal radiation. A fireball occurs when there is immediate ignition of a pressurised release of flammable material in the event of a vessel or pipeline failure. A jet fire can occur underneath a fireball and remain after the fireball has dissipated, or if ignition is delayed.

This report describes a literature review of models that estimate the thermal radiation hazards, as well as experimental data that can be used to validate the models. The report details the different techniques available and any pipeline experimental data that was identified. The report includes identification of areas where there is a large variability in the parameters used in the modelling.

These findings are being used as part of the assessment of whether the fireball and jet fire models HSE currently uses are fit-for-purpose or whether changes would be beneficial.

This report and the work it describes were funded by the Health and Safety Executive. Its contents, including any opinions and/or conclusions expressed, are those of the authors alone and do not necessarily reflect HSE policy.

Radiation calculations for fireball and jet fire models: A literature review

**Zoe Chaplin
Andy Jackson**

Health and Safety Executive
Harpur Hill, Buxton, SK17 9JN

Key Messages

Methodologies and data to model the effects of thermal radiation from jet fires and fireballs have been reviewed. The Health and Safety Executive (HSE) model the consequences of a fireball and jet fire when assessing the hazards associated with major hazard sites and major accident hazard pipelines. The review of fireball and jet fire models has been undertaken as part of the continuous improvement of models in HSE, in particular, in relation to the ongoing development of HSE's pipeline risk assessment model, MISHAP.

A literature search was undertaken to investigate models that estimate the thermal radiation hazards. The literature search also identified experimental data that can be used to validate any thermal radiation model.

There are two main techniques for modelling thermal radiation that are used within the literature. The first of these is the point source technique, or, with a modification, the multiple point source technique. This assumes that the fire radiates from a single point (or multiple points). It is generally considered to be less accurate than other techniques in the region near the fire. It also requires knowledge of the fraction of heat radiated, that is, the fraction of the radiation that is emitted as heat. Several correlations have been derived in the literature for this parameter from generally small scale experiments. The correlations are specific to the set of experiments used to derive them.

The second methodology is the solid flame technique. This method treats the flame as a solid body that radiates heat from all parts of the flame. It requires knowledge of the geometry of the flame as well as either the flame temperature or the surface emissive power (SEP), and the atmospheric transmissivity, that is, how effectively the radiation spreads through the atmosphere. The literature and experimental data has shown wide variation in the values of the SEP, but it has been shown to vary largely according to the substance that is being burnt. Some agreement can be found on the approximate value of the SEP for specific substances.

From reviewing the literature, it has been found that different techniques have been used to estimate the atmospheric transmissivity but it is often unclear how these have been derived. One method appears to be more widely used and the data on which it is based is available in the literature.

There is limited data available from experiments, particularly for pipelines. The data show wide variation in the values of parameters such as the SEP, often depending on exactly where it is measured and what is being reported (e.g. maximum values, average values, from the top, bottom or middle of the fire etc.).

This review is being used to inform the next phases of work, which will determine whether the existing HSE jet fire and fireball models are fit-for-purpose or whether it would be beneficial to make changes to the models.

Executive Summary

Background

The Health and Safety Executive (HSE) is a statutory consultee for Land Use Planning (LUP) developments near Major Accident Hazard (MAH) pipelines that fall under the Pipelines Safety Regulations (PSR).

The MISHAP (Model for the estimation of Individual and Societal risk from Hazards of Pipelines) model is used by HSE to calculate the risks associated with MAH pipelines in Great Britain. The risk levels calculated are used by HSE to determine the distances to LUP zones around the MAH pipeline.

As part of the Quantitative Risk Assessment (QRA) process, MISHAP models fireballs and jet fires as a consequence of a flammable release from a MAH pipeline. For substances other than natural gas, MISHAP additionally models the effects of a flash fire in conjunction with a jet fire.

MISHAP contains one fireball model for all substances and two jet fire models: a model for natural gas pipelines; and a model for all other flammable substances.

Aims

MISHAP has been undergoing a programme of updates and improvements. As part of this improvement programme, the fireball model and the two jet fire models in MISHAP have been reviewed and compared against other published models. This has been to establish whether the current models are fit-for-purpose, or whether there are improved models available that could be implemented within MISHAP.

In addition, the literature has been investigated to determine if there is any experimental data that can be used to validate the models in MISHAP or any new proposed models. The identified models and data have been reported as part of an earlier stage of this work.

Findings

The fireball model in MISHAP is a simple model that assumes the fireball grows instantly to its maximum size and never rises above the ground. After a determined time (not more than 30 s), the fireball instantly dissipates into the surrounding atmosphere. The fireball is assumed to radiate heat at a constant rate for its entire duration. The same model is used by HSE to model fireballs resulting from failure of static vessels.

The jet fire model used within MISHAP for releases of natural gas is a simple model adopted many years ago and seems to be limited by the computational power that was

available at that time. It cannot model the effects of wind or angle of tilt on the calculated flame length and trajectory.

The jet fire model used within MISHAP for releases of other substances is more sophisticated than that used for natural gas releases. It can be used to model single or two-phase flows, as well as being able to model the effects of wind or angle of tilt on the calculated flame length and trajectory.

Both of the existing jet fire models within MISHAP assume that the fireball has already dissipated, i.e. the early stages of a release are not modelled. MISHAP separately models the effects of the fireball that may form following a release, but does not include the jet fire at this stage. The physical reality is that the fireball and jet fire will form concurrently following a release following immediate ignition, with the unburned material in the jet fire feeding the fireball as it rises from ground level. The fireball will then dissipate while the jet fire continues to burn for a longer time period.

The current work details the results of a literature search on the calculation of thermal radiation from fireballs and jet fires. As well as considering theoretical models, the literature review also aimed to identify any suitable data that could be used to validate the existing models and/or any revised models.

It was found that there are two primary ways of calculating the thermal radiation from fires. The first treats the fire as a point source i.e. the heat is radiated from a single point. This does not consider the geometry of the fire. A slight modification to this method is to treat the fire as a multiple point source radiator. The second method is the solid flame technique. This method includes the geometry of the fire and is considered to be more accurate than the point source method, particularly close to the fire where the shape of the flame is of greater importance.

In the point source method it is necessary to estimate the fraction of the total heat that is radiated by the fire. Correlations have been derived for this based on generally small scale data. The solid flame technique requires knowledge of the surface emissive power of the flame, the atmospheric transmissivity and the view factor. Various different methods have been identified to calculate each of these properties.

Conclusions

It is recommended that the results of the literature review are used to inform future decisions regarding modifying or rewriting the fireball model for pipelines and/or static sites. It should also be used to inform future decisions concerning the development of the jet fire model in MISHAP.

Contents

Key Messages	4
Executive Summary	5
1 Introduction	8
1.1 Background	8
1.2 Research aim	9
1.3 Structure of report	10
2 Current radiation calculations	11
2.1 Fireball model description	11
2.2 Discussion	12
2.3 Jet fire model description	12
2.4 Discussion	17
3 Literature on radiation calculations	18
3.1 Fireballs	18
3.2 Jet fires	28
3.3 Fireballs and jet fires	45
3.4 Discussion	59
4 Conclusions	71
5 References	72

1 Introduction

1.1 Background

The Health and Safety Executive (HSE) provide land-use planning (LUP) advice to local authorities for major hazards sites [1] and pipelines. Under the Planning (Hazardous Substances) Regulations [2], the presence of hazardous chemicals above specified threshold quantities requires consent from a Hazardous Substances Authority (HSA). HSE is a statutory consultee on all Hazardous Substances Consent (HSC) applications. Its role is to consider the hazards and residual risk which would be presented by the hazardous substance(s) to people in the vicinity, and on the basis of this to advise the HSA whether or not consent should be granted.

A Hazardous Substances Consent assessment relating to flammable substances considers a number of possible flammable hazards, including a fireball and a jet fire. A fireball occurs when a release of flammable material is ignited immediately upon vessel failure. A fireball is approximately spherical in shape and grows rapidly, before rising due to buoyancy. It is highly transient, normally lasting only a few seconds.

A jet fire can occur underneath a fireball, or on its own following delayed ignition of a flammable substance. If there is delayed remote ignition and the substance is not lighter than air, then a flash fire can also be formed with a jet fire. The jet fire can reach an approximate steady state after a relatively short period of time, where the average flame length and width are unvarying with time. HSE assesses the thermal radiation hazard posed to people from a fireball and a jet fire and these calculations are used to generate LUP zones around the site.

Fireballs and jet fires are also considered in the assessment of LUP zones in the vicinity of Major Accident Hazard (MAH) pipelines. HSE is a statutory consultee for MAH Pipelines, which fall under the Pipeline Safety Regulations (PSR) [3]. HSE considers the risks to people in the vicinity of the pipeline, and provides advice accordingly. Consultation is required for new pipelines, modifications to existing pipelines, and to new developments in the vicinity of an existing pipeline. The fireball and jet fire are considered in conjunction with weather data, failure frequencies and the outputs from other consequence models to generate the LUP zones around the pipeline.

The existing fireball model used by HSE for both HSC applications and MAH pipelines is called FBALL and is based on work by Roberts [4]. It is a simple model that assumes the fireball grows instantly to its maximum size and never rises above the ground. After a determined time (not more than 30 s), the fireball instantly dissipates into the surrounding atmosphere. The fireball is assumed to radiate heat at a constant rate for its entire duration.

HSE decided that the fireball model required reviewing, and that the literature should be investigated to determine what information was available on the subject. The review should cover both static sites and pipelines. For static sites, following a catastrophic failure of a vessel and immediate ignition, a fireball is formed that dissipates within a few seconds. In this case, the main force acting to make the fireball rise is buoyancy. For pipelines, a continual supply of pressurised fluid emerges from the failure point, which can either be a leak or a rupture. Assuming that the fluid immediately ignites on pipeline failure, a fireball forms with a jet fire below it. The continuous supply of fluid feeds the jet fire and the unburned material in the jet fire feeds the fireball above it. The fireball dissipates after less than 30 s, leaving the jet fire behind. In this scenario, the main force acting to make the fireball rise is momentum.

In conjunction with the review of fireball modelling, HSE decided that the jet fire models within MISHAP also required reviewing. MISHAP contains two jet fire models; a model for releases from natural gas pipelines and a model for all other substances. The models were written in the 1990s and early 2000s and contain a number of approximations.

The literature review for fireballs was divided into two stages. The first investigated the physical dimensions of the fire and its behaviour [5]. It included the identification of any experimental data that could be used to validate any models implemented within MISHAP. For the jet fires, the review was divided into three stages. The first considered the physical dimensions of the fire [6] and available data, and the second compared the performance of several models from the literature with the identified data [7]. This report is concerned with the second stage of the fireball review and the third stage of the jet fire review, which considers the calculation of the thermal radiation.

Aspects of the thermal radiation calculations are similar for both fireballs and jet fires. This report therefore considers the modelling of thermal radiation from both types of fire. This is particularly relevant to the pipeline fireball modelling scenario where a jet fire underlies the fireball.

1.2 Research aim

The objectives of the work were:

- To identify and describe literature pertaining to the modelling of thermal radiation from fireballs and jet fires;
- To use the literature review to inform a decision regarding what method should be used for a revised fireball model;
- To use the literature review to inform a decision regarding what method should be used for a revised jet fire model;
- To identify any data, additional to that identified in Stage 1 of the fireball and jet fire model reviews, which could be used to validate the thermal radiation aspects of a revised fireball model or jet fire model.

1.3 Structure of report

The remainder of the report is structured as follows:

- Section 2 describes the current radiation calculations within the fireball model and the jet fire models;
- Section 3 describes the literature review; and
- Section 4 presents the conclusions and recommendations.

2 Current radiation calculations

2.1 Fireball model description

HSE's current fireball model, FBALL, is based on work by Roberts [4] and assumes that the fireball radiates at a constant value throughout its duration. The radiation heat flux (I , kW m⁻²) is calculated by:

$$I = E\tau F \quad (1)$$

where:

- E = the surface emissive power (kW m⁻²);
- τ = the transmissivity of the atmosphere; and
- F = the view factor.

The surface emissive power (SEP) is assumed to be the same for all substances and for both pipelines and vessels. It is set at a value of 270 kW m⁻² for fireballs of less than 125 tonnes, and to 200 kW m⁻² otherwise. These values are based on propane fireballs but are used for all substances. A formula is also given to allow for modifications in the case of vessels, if required, based on the burst pressure of the vessel (P , MPa). This formula is given as:

$$E = 235P^{0.39} \quad (2)$$

The view factor, F , is calculated using:

$$F = \frac{\frac{x}{r}}{\left(\left(\frac{x}{r}\right)^2 + 1\right)^{\frac{3}{2}}} \quad (3)$$

where x (m) is the distance of the target from the pipeline break point and r (m) is the fireball radius.

The transmissivity, τ , of the atmosphere is calculated as:

$$\tau = 1 - 0.009293(\ln(x))^{1.389} \varphi^{0.2868} \quad (4)$$

where φ is the relative humidity (%) and x (m) is the distance of the target from the pipeline break point.

2.2 Discussion

The values for the surface emissive power are stated to be based on propane fireballs and are used for all substances. The derivation of the surface emissive power values was made many years ago and its exact origin is uncertain.

The view factor calculation is a standard calculation for a sphere. It does, however, assume that the fireball is on the ground throughout its duration.

The origins of the atmospheric transmissivity calculation are unclear. It is understood that the correlation was derived using experimental work on pool fires and comparing this with atmospheric transmissivity curves in the wider literature. No documentation has been obtained to definitively state how it was derived, however.

2.3 Jet fire model description

There are two jet fire models in MISHAP. The first of these, PIPEFIRE, is for natural gas fires only. The second, JIF/MAJ3D, is for single and two-phase flows of all other substances.

2.3.1 PIPEFIRE

PIPEFIRE consists of two models; a trench-fire model for ruptures and a jet fire model for all other hole sizes. The flame is insensitive to the wind in both models. A full description of both models is given in Chaplin [8] but the aspects specific to the radiation are discussed subsequently. In both models, the solid flame technique is used to calculate the incident radiation, I (kW m^{-2}):

$$I = E\tau F \quad (5)$$

where:

- E = the surface emissive power (kW m^{-2});
- τ = the transmissivity of the atmosphere; and
- F = the view factor.

TRENCH-FIRE MODEL

The trench-fire model considers the flame to be a vertical rectangular sheet of flame. It is assumed that a person or building is at a horizontal distance, D (m), from the centre of the base of the sheet. The various distances used in the view factor calculation are shown in Figure 1.

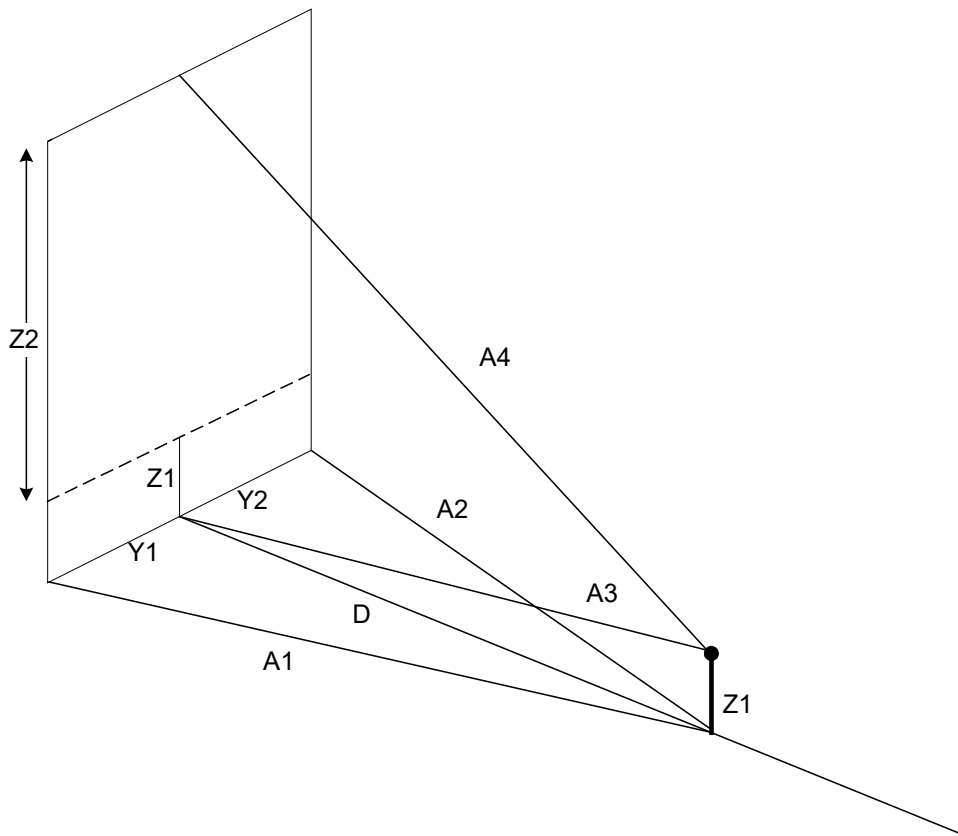


Figure 1 Diagram of the trench-fire view factor

Y1 and Y2 are set to half the flame width. Z1 is the receiver height (either building height or human height) and Z2 is the height of the flame minus Z1. The various distances are calculated as follows:

$$A1 = A2 = \sqrt{Y1^2 + D^2} \quad (6)$$

$$A3 = \sqrt{Z1^2 + D^2} \quad (7)$$

$$A4 = \sqrt{Z2^2 + D^2} \quad (8)$$

The view factor is given by:

$$F = \frac{F1 + F2 + F3 + F4}{2\pi} \quad (9)$$

where:

$$F1 = \frac{Y2}{A2} \left(Atn \left(\frac{Z2}{A2} \right) + Atn \left(\frac{Z1}{A2} \right) \right) \quad (10)$$

$$F2 = \frac{Y1}{A1} \left(Atn \left(\frac{Z2}{A1} \right) + Atn \left(\frac{Z1}{A1} \right) \right) \quad (11)$$

$$F3 = \frac{Z2}{A4} \left(Atn \left(\frac{Y2}{A4} \right) + Atn \left(\frac{Y1}{A4} \right) \right) \quad (12)$$

$$F4 = \frac{Z1}{A3} \left(Atn \left(\frac{Y2}{A3} \right) + Atn \left(\frac{Y1}{A3} \right) \right) \quad (13)$$

and Atn is the arctangent.

The surface emissive power, E , is set to 256 kW m⁻². The atmospheric transmissivity, τ , uses a British Gas correlation which is said to correspond to an atmospheric relative humidity of 50% (note that this is lower than the 60% HSE standard value of relative humidity):

$$\tau = 1 - 0.058 \ln(x) \quad (14)$$

where x (m) is the distance from the flame to the receiver.

JET FIRE MODEL

The jet fire model is assumed to be a cylinder and the view factor is calculated using the standard expressions for a cylindrical emitter. The surface emissive power is set to 300 kW m⁻² for all three hole sizes (large, small and pin) and the atmospheric transmissivity is given by Equation 14.

2.3.2 JIF/MAJ3D

JIF calculates the length of the jet flame and MAJ3D performs the radiation calculations. The flame is assumed to be a conical shaped (frustum) solid radiator with a uniform emissive power. Unlike PIPEFIRE, the jet is affected by the wind speed. The geometry of the flame relative to the pipeline is shown in Figure 2.

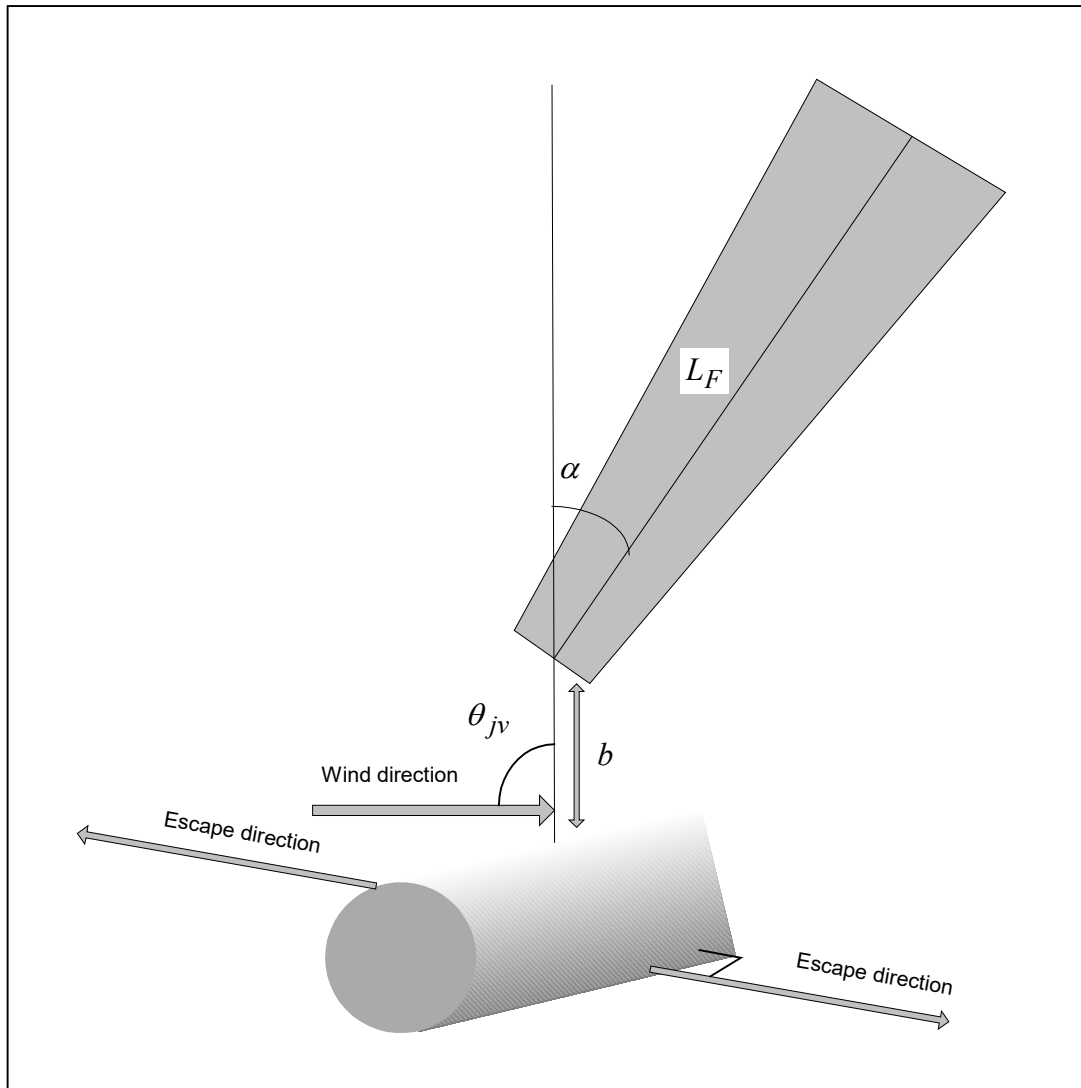


Figure 2 Diagram of the geometry of the jet fire in JIF/MAJ3D

In Figure 2, α ($^\circ$) is the angle of tilt of the jet, L_F (m) is the frustum length, b (m) is the frustum lift-off length and θ_{jv} ($^\circ$) is the angle between the hole axis and the wind vector (set to 90° in MISHAP).

To calculate the thermal radiation flux, the jet is treated as a 4-point radiator with points on the flame axis located at 0.3, 0.5, 0.7 and 0.9 of the flame length. The fractions of the total heat radiated by the jet, F_{Hrad} , that are associated with these points are:

$$F_{Hrad} = 0.4787 \text{ when } X = 0.9L_F \quad (15)$$

$$F_{Hrad} = 0.2978 \text{ when } X = 0.7L_F \quad (16)$$

$$F_{Hrad} = 0.1596 \text{ when } X = 0.5L_F \quad (17)$$

$$F_{Hrad} = 0.0639 \text{ when } X = 0.3L_F \quad (18)$$

where X (m) is the distance of the point source along the jet.

The total heat released by the jet, H_{rel} ($J s^{-1}$), is a product of the heat of combustion, ΔH_c ($J kg^{-1}$), with the mass flow rate (taken at 30 s in MISHAP), G ($kg s^{-1}$), calculated by the release rate model:

$$H_{rel} = G\Delta H_c \quad (19)$$

The total amount of heat radiated, H_{rad} ($J s^{-1}$, or W), is a fraction of the total heat generated by burning the fuel:

$$H_{rad} = fH_{rel} \quad (20)$$

where f is the radiated heat fraction given by [9]:

$$f = 0.21e^{-0.00323u} + 0.11 \quad (21)$$

for single phase jets, and u_j ($m s^{-1}$) is the expanded jet velocity. For two-phase jets, f is set to 0.38.

The heat radiated at each of the point sources, PS ($J s^{-1}$, or W), is then given by:

$$PS = H_{rad}F_{Hrad} \quad (22)$$

The flux, I ($kW m^{-2}$), at any given distance is given by:

$$I = \sum_{radiators=1}^4 \frac{PS\tau}{4\pi x_p} \quad (23)$$

where:

- x_p = the distance (m) from the target to the point radiator given by:

$$x_p = \sqrt{\left(X\sin\left(\frac{\alpha\pi}{180}\right) - x_d\cos(\lambda)\right)^2 + (x_d\sin(\lambda))^2 + \left(X\cos\left(\frac{\alpha\pi}{180}\right) - y_d\right)^2} \quad (24)$$

- X = the distance (m) along the jet for the point source, given in Equations 15 to 18;
- x_d = the horizontal distance (m) from the target to the jet;
- λ = the angle (radians) between the target and the jet (set to 0 or π radians (0° or 180°) as it is assumed that the jet is either angled towards the target or away from the target, and the target runs away in a direction perpendicular to the pipeline i.e. parallel to the jet flame);
- y_d = the target height (set to the human target height, which, by default is 2 m): and
- τ = the atmospheric transmissivity, given by:

$$\tau = 1 - 0.009293(\ln(x))^{1.389} \varphi^{0.2868} \quad (25)$$

where φ is the relative humidity (%), normally 60%, and x (m) is the distance of the target from the pipeline break point.

2.4 Discussion

2.4.1 PIPEFIRE

The values for the surface emissive power and the atmospheric transmissivity were derived many years ago and there is a degree of uncertainty around their origins. The view factors for both the trench-fire model and the jet fire model, on the other hand, use standard equations from the literature.

2.4.2 JIF/MAJ3D

The equation for the atmospheric transmissivity is the same as that used in the fireball model. As has already been discussed (paragraph 18), the origins of the equation are unclear although it is believed to be based on some experimental pool fire data.

The equation for the fraction of heat radiated used for single-phase jets has been taken from work by Chamberlain [9]. The value of 0.38 used for two-phase jets, however, is thought to be based on internal discussions with Chamberlain. The intention appears to have been to use this value unless specific information was available.

3 Literature on radiation calculations

A literature search was conducted to identify any information on methods for the calculation of radiation from fireballs and jet fires. A large number of references were identified as being of possible relevance, each of which will be discussed subsequently. The literature has been divided into different sections depending on whether it is purely considering fireballs or jet fires, or whether it is applicable to both types of fire.

3.1 Fireballs

3.1.1 Fay et al., 1979 [10]

The paper looks at the measurement and analysis of time resolved thermal radiation from experiments using methane, ethane and propane and follows on from earlier work in the field [11]. The experiments were small scale, with initial fuel volumes of between 20 cm³ and 200 cm³. The vapour samples were initially contained within a spherical soap film. The film was broken by touching it with a hot wire, which started the combustion process. The gas burned as an unsteady turbulent diffusion flame.

The authors state that there is some uncertainty around extrapolation of the results to much larger fireballs.

3.1.2 Roberts, 1981 [4]

The author considers LPG fireballs from pressurised storage. Using data obtained from the experiments of Hasegawa and Sato [12], the author derives a correlation for the fraction of the combustion energy that is radiated as thermal radiation (fraction of heat radiated) from the fireball, f , in terms of the burst pressure, P (MPa):

$$f = 0.27P^{0.32} \quad (26)$$

The burst pressures in Hasegawa and Sato's work only went to approximately 1.5 MPa. Roberts extrapolates up to a pressure of 6 MPa.

3.1.3 Williamson and Mann, 1981 [13]

The paper aims to describe a thermal radiation model for LPG fireballs. It uses the assumption that the fireball radius grows in proportion to the cube root of time, which allows an equation for the heat flux to be derived. The equation is dependent on the radius at the point the fireball lifts off, the thermal flux at the fireball surface, the distance of the object from the fireball centre, and the mass of fuel. The thermal flux at the fireball surface requires the fireball flame temperature to be known.

A number of assumptions have been made to derive the model. These are:

- The rate of propane addition to the fireball is constant;

- A stoichiometric mixture is assumed to exist at ignition;
- All of the available fuel participates in the reaction;
- The fireball is an isothermal, spherical, homogeneous body at all times;
- The fireball radiates as a black body;
- Fuel burnout time and lift-off time coincide; and
- The absorbed heat flux is approximately the same as the incident heat flux.

The authors acknowledge that the model can only provide an estimate of the potential hazards posed by a fireball due to the lack of experimental data.

3.1.4 Lihou and Maund, 1982 [14]

The authors consider the results of small scale fireball tests. They quote a correlation for the incident thermal flux density, I (kW m⁻²) that will cause severe blistering, based on the work of Stoll and Chianta [15]:

$$I = \frac{50}{t_d^{0.71}} \quad (27)$$

where t_d is the fireball duration (s).

An alternative equation is given for Boiling Liquid Expanding Vapour Explosions (BLEVEs) of glass vessels at 15 m range, based on the mass, m (kg):

$$I = 3.1m^{0.661} \quad (28)$$

After reviewing equations from the literature, the authors derive their own expression, based on the Stefan-Boltzmann law i.e.:

$$I = \tau EF \quad (29)$$

where:

- τ = atmospheric transmission coefficient;
- E = flame surface emissive power (kW m⁻²); and
- F = view factor between flame and receiver.

For the atmospheric transmissivity, τ , the authors use:

$$\tau = \exp(-7 \times 10^{-4} S) \quad (30)$$

where S (m) is the distance from the edge of the fireball to the target area and assuming a visibility constant of 0.7. It is not clear how this equation has been derived, although an equivalent equation has been found in Satyanarayana et al [16] (section 3.3.5).

3.1.5 Moorhouse and Pritchard, 1982 [17]

The authors review methods used to calculate the thermal radiation from pool fires and fireballs. They first discuss general methods, i.e. the point source technique and the solid flame technique. The point source technique does not consider the flame geometry but instead assumes that the fire radiates from a single point. The general form of the technique is given by:

$$I = \frac{fmH_c}{4\pi S^2 t} \quad (31)$$

where:

- I = intensity of incident thermal radiation (kW m⁻²);
- f = fraction of heat of combustion of fuel that is radiated;
- m = mass of fuel (kg);
- H_c = heat of combustion (kJ kg⁻¹);
- S = distance from flame or fireball centre to receiving surface (m); and
- t = time (s).

The authors point out two limitations of the point source technique. The first of these is that it is assumed that receiving surfaces are always considered to be inclined towards the flame such that they receive the maximum incident flux. In reality, this is not the case for buildings or tanks.

The second limitation is that it does not provide an accurate calculation for objects that are relatively close to the fire as the flame geometry is of more importance in this region. For these reasons, the authors state that the point source technique is not recommended for use. As fireballs are approximately spherical, however, the authors state that the method may be a reasonable approximation for this type of fire.

One way of overcoming the limitations of the point source technique is to consider multiple point sources. Each point consumes a proportion of the fuel and each contributes to the radiation received by the target. This method takes more account of the geometry of the flame but can become complex when considering the orientation of the receiver. It can therefore be simpler to consider the flame as a solid geometrical shape i.e. using the solid flame model, which, in general terms, is given by:

$$I = \tau EF \quad (32)$$

where:

- I = intensity of incident thermal radiation (kW m^{-2});
- τ = atmospheric transmission coefficient;
- E = flame surface emissive power (kW m^{-2}); and
- F = view factor between flame and receiver.

In the solid flame technique, it is assumed that a flame can be represented by a solid shape which radiates heat as a consequence of its high temperature.

Published information on the parameters for the solid flame technique for pool fires and fireballs is reviewed. As it is fireballs that are of most interest in this report, it is this information that will be covered subsequently.

In general terms, the surface emissive power, E (W m^{-2}), is related to the flame temperature, T_f (K), and the flame emissivity, ε , according to:

$$E = \varepsilon \sigma T_f^4 \quad (33)$$

where σ is the Stefan-Boltzmann constant ($5.670373 \times 10^{-8} \text{ W m}^{-2} \text{ K}^{-4}$).

For fireballs, the flame temperature is often not known and the authors state that information on SEP is limited. Values and equations quoted in the literature have been based on small scale experiments. Significant variation in the SEP was seen from test to test, which may be due to the effects of wind. The authors derive a correlation for the SEP based on the fuel pressure, P (MPa), but this is only applicable for fuel masses of 6.2 kg:

$$E = 235P^{0.39} \quad (34)$$

The authors state that there is insufficient available information to select accurate values for the SEP for fireballs. They state that, for pure vapour fireballs, a realistic minimum is about 150 kW m^{-2} and the maximum value is unlikely to exceed 300 kW m^{-2} . This is based on the small scale experiments of Hasegawa and Sato [12], however, and may not be appropriate to the orders of magnitude larger fireballs of interest in this report.

Moorhouse and Pritchard ultimately consider the point source technique to derive the incident thermal radiation. They use correlations for the diameter and duration to derive an equation for the fraction of heat radiated, f :

$$f = \frac{\pi E}{H_c} \quad (35)$$

Some consideration is given to the atmospheric transmittance. Values are given for the transmission coefficients based on the available literature. No specific equation or values are suggested, but the authors state that the coefficients should be “appropriate to the type

of combustion event considered” and “the path length chosen for absorption should be representative of that from the receiver to the flame surface and not based on the ground separation distance”.

3.1.6 Simpson, 1984 [18]

This report contains a number of graphs of atmospheric transmissivity by distance, obtained from different sources in the literature and using varying assumptions. It is thought that the correlation currently used for atmospheric transmissivity for fireballs by HSE (Equation 4 in Section 2.1) was derived using these curves.

3.1.7 Partanen and Vuorio, 1985 [19]

The paper is concerned with LPG BLEVEs and, in particular, the cooling of the fireball by radiation and by mixing with the surrounding air. It was found that the dominant cooling mechanism for LPG fireballs is the entrainment of cold air, which also determines the duration of the fireball.

Small scale experiments from elsewhere in the literature (e.g. Fay and Lewis [11], Lihou and Maund [14]) were investigated. From the experiments it was shown that an upper bound to the amount of radiation from a small propane fireball is 25% of the total energy released. This appears to validate the assumption that radiation is not the main cause of cooling of LPG fireballs. Two models to determine the accuracy of the assumption are described. The first assumes cooling by mixing only and the second by radiation only.

The simple models indicate that the mixing with the surrounding air cools the fireball rapidly. Radiative cooling, in contrast, leads to much smaller changes in the fireball temperature. Further analysis leads the authors to conclude that the thermally radiated energy is proportional to the 5/6th power of the fuel mass. This only applies to optically thick fireballs, such as LPG.

It should be noted that only data from small scale experiments has been considered in this paper.

3.1.8 Clay et al., 1988 [20]

In this paper, the incident radiation is calculated using the solid flame technique (i.e. Equation 32, Page 21). The surface emissive power of the fireball, E (kW m⁻²), is given by a correlation on the burst pressure, P (MPa), which was taken from Moorhouse and Pritchard [17] and is applicable for fuel masses up to 6.2 kg:

$$E = 235P^{0.39} \quad (36)$$

The value of the pressure is normally taken as the relief valve setting. The authors state that it is assumed to be 1.45 MPa for propane and 0.52 MPa for butane.

The atmospheric transmissivity, τ , is based on the distance from the fireball to the receiver (S , m), and is given by:

$$\tau = 1 - 0.0565 \ln(S) \quad (37)$$

The authors state that the fireball model is based on the work of Roberts [4] and Fay and Lewis [11]. As neither of the equations quoted here can be found in either of these two papers, it is believed that the authors are referring to the equations for the fireball dimensions, rather than the radiation aspects. It is therefore not clear how the correlation for the atmospheric transmissivity has been derived.

3.1.9 Johnson and Pritchard, 1991 [21]

In this paper, the results of five large scale BLEVE experiments are reported. Three of the experiments involved 2 tonnes of butane, one involved one tonne of butane and the fifth experiment used 2 tonnes of propane.

The surface emissive power of the fireballs was measured. It was found that peak values of up to 500 kW m⁻² were recorded at the top of the expanding fireball. The remainder of the fireball radiated at values of between 250 and 350 kW m⁻². The average SEP calculated for each experiment ranged from 306 kW m⁻² to 368 kW m⁻². These values are consistent with the value of 340 kW m⁻² suggested for propane in Croce and Mudan [22] and are similar to the value of 380 kW m⁻² suggested for butane (section 3.3.1).

3.1.10 Prugh, 1994 [23]

This paper considers the hazards associated with fireballs. The author states that the thermal radiation received by a target is a strong function of the thermal radiation intensity, I (kW m⁻²), at the surface of the fireball:

$$I = \sigma \varepsilon (T_f^4 - T_r^4) \quad (38)$$

where:

- ε = flame emissivity (kW m⁻²);
- σ = the Stefan-Boltzmann constant (5.670373×10^{-11} kW m⁻² K⁻⁴);
- T_f = temperature at the surface of the fireball (K); and
- T_r = temperature of the receptor (K).

A value of 1.0 for the flame emissivity is chosen if the diameter of the fireball is greater than 3 m and it is not transparent (i.e. the fireball can be described as “optically thick”).

The colour of the fireball flame provides an indication of the flame temperature, which can range from approximately 1120 K to 1370 K. The authors state that fireballs are normally at the upper end of this range, at which point the temperature of the receiver becomes relatively insignificant. Using these assumptions, Equation 38 becomes:

$$I = 5.67 \times 10^{-11} T_f^4 \quad (39)$$

The author states that the thermal radiation at the surface of a fireball would be of the order of 200 kW m⁻². The temperature of the fireball (°C) can be calculated from:

$$T_f = \left(\frac{H_c}{C_p} \right) + T_0 \quad (40)$$

where:

- H_c = heat of combustion of the fuel (cal g⁻¹);
- C_p = heat capacity of the combustion products (cal g⁻¹ °C⁻¹); and
- T_0 = average temperature of the fuel and of the surrounding air (°C).

A discussion is given on the reasons that the flames are usually yellow or orange (i.e. temperatures ranging between 1220 K and 1520 K), which allows radiation fractions of between 0.25 and 0.40 to be inferred. These include non-stoichiometry (insufficient oxygen and combustion to carbon monoxide rather than carbon dioxide) and loss of heat by convection.

Later in the paper an equation is given for the fractional atmospheric transmissivity, τ :

$$\tau = \frac{1.30}{(P_w R_T)^{0.09}} \quad (41)$$

where:

- P_w = partial pressure of water (mm Hg); and
- R_T = distance to the surface of the fireball (m) given by:

$$R_T = S - \frac{D_{max}}{2} \quad (42)$$

- S = distance from the centre of the fireball to the receptor (m); and
- D_{max} = maximum diameter of the fireball (m).

The reference for the transmissivity equation is given as a CCPS book. The later edition of the book [24], however, does not contain the equation and only refers to that from the “Yellow Book” [25] which is very similar to Equation 41.

3.1.11 Makhviladze et al., 1999 [26]

The authors use the model of the Weighted Sum of Grey Gases (WSGG) to calculate the optical properties of the combustion products of hydrocarbon fuels. In the WSGG, the emissive power is approximated by the sum of the emissive powers of a set of grey gases, each of which has an intrinsic absorption coefficient, κ_j . The summation is performed over temperature dependent weighting coefficients, α_j . The coefficients, α_j , can be thought of as the total contribution to the radiation from all regions of the spectrum in which the absorption coefficients are close to κ_j .

The authors consider three grey gases (water vapour and two mixtures of water vapour and carbon dioxide) together with mixtures of the radiating gases and soot. The coefficients required in the calculations have been obtained from the wider literature.

The radiant energy flux, I_R ($W\ m^{-2}$) is the sum of the individual fluxes, I_{Rj} ($W\ m^{-2}$), given by:

$$I_R = \sum_{j=1}^{\kappa} I_{Rj} \quad (43)$$

where each of the individual fluxes is given by:

$$\nabla I_{Rj} = \kappa_j (\alpha_j E_b - E_j) \quad (44)$$

where:

- E_b = radiation density of an ideal black body ($W\ m^{-2}$) i.e.

$$E_b = 4\sigma T^4 \quad (45)$$

- E_j = volumetric density of the radiant energy of the j th grey gas ($W\ m^{-2}$); and
- σ = the Stefan-Boltzmann constant ($5.670373 \times 10^{-8}\ W\ m^{-2}\ K^{-4}$).

The authors suggest approximations to calculate the individual fluxes in Equation 44, and hence the total radiant energy flux.

A Monte Carlo method was utilised to calculate the radiation field outside the fireball.

The authors report the fraction of energy converted to radiation from their calculations. The values depend on the mass of fuel involved (ranging from 1 g to 1000 kg). The lowest values are seen for the largest fuel masses (0.17 to 0.2). This is because, for large, optically thick fireballs, the radiation is mainly emitted from the surface of the fire. As the fireball dimensions increase, the radiative heat fraction decreases.

The largest values of fraction of heat radiated are found for the intermediate fireballs (masses of 50 g to 1 kg). The fireball dimensions are of the order of several metres for these masses and the fractions of heat radiated range from 0.24 to 0.27. Fireballs at smaller dimensions are optically thin, which reduces the emissive power. For the smallest fireballs (1 g) the fraction of heat radiated ranges from 0.21 to 0.25. It is stated that the range of values, from 0.17 to 0.27, agrees well with measurements in the literature [27, 28] (sections 3.2.1 and 3.2.6).

3.1.12 Martinsen and Marx, 1999 [29]

The authors propose a dynamic model for fireballs. The fireball is assumed to grow at a rate proportional to the one third power of time during the first third of its duration, t_d (s). After that, the diameter of the fireball remains static but it starts to rise from the ground at a constant rate. Its centre reaches a maximum height of three times its maximum radius at time t_d .

The thermal radiation incident upon a target, I (kW m^{-2}), is given by the standard solid flame model i.e.

$$I = EF\tau \quad (46)$$

where:

- E = average radiant heat flux emitted from the surface of the fireball (kW m^{-2}) i.e. the surface emissive power;
- F = the view factor from the target to the fireball; and
- τ = the atmospheric transmittance.

The surface emissive power, E (kW m^{-2}), of the fireball is given by:

$$E = \frac{fmH_c}{0.8888\pi D^2 t_d} \quad (47)$$

where:

- f = fraction of heat emitted as radiation and is obtained from earlier work in the area [4] which applies to burst pressures up to 6 MPa:

$$f = 0.27P^{0.32} \quad (48)$$

- m = mass of fuel (kg);
- H_c = heat of combustion of the fuel (kJ kg^{-1});
- D = maximum diameter of the fireball (m);
- t_d = fireball duration (s);
- $0.8888\pi D^2$ = time-averaged surface area of the fireball (m^2); and
- P = the burst pressure (MPa).

The SEP calculated in this manner is applied to the fireball during its growth phase. During the remaining 2/3 of its duration, the SEP decreases linearly to zero.

The view factor is given by standard equations for a sphere radiating to a point outside the sphere. The atmospheric transmittance is given by the equations from Wayne [30] (section 3.3.6).

3.1.13 Roberts et al., 2000 [31]

The paper reports the results of a series of experiments on 2 tonne propane vessels. A table is given of average surface emissive powers and maximum SEPs from the fireballs.

The average values ranged from approximately 240 kW m⁻² to 400 kW m⁻², and the maximum SEP values ranged from 480 kW m⁻² to 650 kW m⁻².

Fractions of heat radiated are calculated using the equation on burst pressure from Roberts [4]. This gives values in the range 0.25 to 0.4.

3.1.14 Novozhilov, 2003 [32]

The paper considers the mathematical modelling of fireballs. A radiation transfer equation (RTE) is used. The radiation intensity, I (W m⁻²), is assumed to change with distance, x (m):

$$\frac{dI(x)}{dx} = -(\alpha_g + \alpha_s)I(x) + \frac{\sigma}{\pi}(\alpha_g + \alpha_s)T_f^4 \quad (49)$$

where:

- α_g = absorption coefficient due to the gas phase;
- α_s = absorption coefficient for soot;
- σ = the Stefan-Boltzmann constant (5.670373×10^{-8} W m⁻² K⁻⁴); and
- T_f = temperature (K).

Correlations can be used for the absorption coefficients.

The authors state that a more comprehensive approach is the use of the weighted sum of grey gases (WSGG) model, which is described in more detail in Makhviladze et al. [26]. It is considered to be more accurate but much less computationally effective.

Later in the paper, the author describes a point source model and a solid flame model to calculate the incident radiation from a fireball.

3.1.15 Abbasi and Abbasi, 2007 [33]

The authors provide a summary of techniques used within the wider literature for the calculation of radiation from BLEVE fireballs. They indicate that some authors using the point source technique actually calculate the SEP, rather than the radiation received by the target (i.e. the distance used is the diameter of the fireball, not the distance to the receiver).

A number of values are quoted from the literature for the fraction of heat radiated, ranging from 0.18 to 0.4. Two equations are given, the first by Roberts [4]:

$$f = 0.25P^{0.32} \quad (50)$$

where:

- f = the fraction of heat radiated; and

- P = vapour pressure at the moment of burst (MPa), $P < 6\text{MPa}$.

Note that Roberts (Equation 26, page 18) uses a constant of 0.27, not 0.25, as quoted in this paper. Equation 50 therefore appears to be in error.

The second equation is from the “Yellow Book” [25] and is the same as Equation 50 but with the constant modified from 0.25 to 0.27 i.e. the same as Roberts. No limit is given on the burst pressure, however.

Two equations are quoted for the atmospheric transmissivity. The first of these is from the CCPS [34] and the “Yellow Book” [25], amongst others, and is given by:

$$\tau = 2.02(P_w S)^{-0.09} \quad (51)$$

where:

- τ = the atmospheric transmissivity;
- P_w = partial water vapour pressure (Pa); and
- S = distance from surface of fireball to the target (m).

The second equation is from the “Yellow Book” [25] and is given by:

$$\tau = 1 - \alpha_w - \alpha_c \quad (52)$$

where:

- α_w = absorption factor for water vapour; and
- α_c = absorption factor for carbon dioxide.

3.2 Jet fires

3.2.1 Markstein, 1976 [27]

The paper reports the results of jet fire experiments using ethane and propane. Both laminar and turbulent flames were observed. The fraction of heat radiated was calculated and shown to vary from approximately 0.2 to 0.25.

3.2.2 Sonju and Hustad, 1984 [35]

This paper reports the results and analysis of experiments on turbulent flames of methane and propane. Thermal radiation fluxes were measured in the experiments. The radiation flux, I (W m^{-2}), was assumed to follow:

$$I = F_{1-2} \langle \varepsilon \sigma T_f^4 \rangle \quad (53)$$

where:

- F_{1-2} = the view factor between the flame and the sensor;
- ε = flame emissivity (W m^{-2});
- σ = the Stefan-Boltzmann constant ($5.670373 \times 10^{-8} \text{ W m}^{-2} \text{ K}^{-4}$); and
- T_f = radiation temperature (K).

The use of Equation 53 allowed the authors to fit correlations to the data for the averaged term in the angled brackets.

3.2.3 Chamberlain, 1987 [9]

Chamberlain considers the thermal radiation from hydrocarbon flares. He states that the thermal radiation, I (kW m^{-2}), can be calculated from:

$$I = \tau EF \quad (54)$$

where:

- F = the view factor;
- E = the surface emissive power (kW m^{-2}); and
- τ = atmospheric transmissivity.

The author states that the view factor can be calculated exactly and that the SEP can be derived empirically. This leads to a revised equation for I of:

$$I = F \times \frac{fQ}{A} \times \tau \quad (55)$$

where:

- f = fraction of heat radiated;
- Q = net heat released by the flame (kW); and
- A = flame surface area (m^2).

The final term in the equation, the atmospheric transmissivity, depends on the concentration of water vapour and carbon dioxide in the atmosphere, and on the distance between the receiver and the flame. The exact equations used to derive the atmospheric transmissivity are not given.

The author uses the results of wind tunnel tests (exit diameters 0.006 to 0.022 m) and field trials (exit diameters 0.152 to 1.07 m) to derive a correlation for the fraction of heat radiated, f , which is dependent on the gas velocity, u_j (m s^{-1}):

$$f = 0.21e^{-0.00323u_j} + 0.11 \quad (56)$$

The fraction of heat radiated decreases with increasing exit velocity due to the fact that, at higher velocities, a greater fraction of heat is lost by convection to entrained air. The laboratory tests used propane and methane whilst the field tests were conducted using vertical releases of natural gas.

Chamberlain derived the surface emissive power from the experiments using the inverse of the equations to calculate the thermal radiation. The SEP for methane was found to vary from 191 kW m⁻² to 254 kW m⁻².

3.2.4 Cook et al., 1987 [36]

This is the first of two papers in which the authors describe field scale experiments of vent stacks of natural gas. The emissive power of the flames is investigated and indicates that the SEP varies considerably with position along the flame locus. The maximum value is located close to the centre of the flare. A mean value across all tests of 239 kW m⁻² was obtained.

Using the emissive power, the authors derive values for the fraction of heat radiated. These are shown to vary from 0.071 to 0.344 with a mean value of 0.187. An alternative method using the observed received radiation has also been used to derive the fraction of heat radiated. In this instance, the values range from 0.076 to 0.338 with a mean of 0.179.

The authors state that the value of the fraction of heat radiated for a particular flare is not just dependent on the fuel being burnt but also on the jet exit velocity and wind speed.

3.2.5 Cook et al., 1987 [37]

In the second of their two papers, the authors describe a mathematical model which has been developed from the results obtained from the field scale experiments detailed in the first paper [36]. The model uses non-dimensional correlations of the experimental data, which they say can be used to predict the length and trajectory of a flare.

The radiation is modelled using a multiple point source model. The experiments indicate that the fraction of heat radiated can be correlated with the jet exit velocity. As the velocity increases, the fraction of heat radiated decreases. A fit to the data yielded a fraction of heat radiated, f , of:

$$f = 0.321 - 0.418 \times 10^{-3}u_j \quad (57)$$

where u_j (m s⁻¹) is the jet exit velocity.

3.2.6 Markstein, 1988 [28]

The paper considers the measurement of radiant emission from laminar hydrocarbon diffusion flames. The experiments were at a small scale, using a burner tube of 4.3 mm internal diameter, 0.15 mm wall thickness and 155 mm in length. A range of hydrocarbons

was considered from C₂H₄ (ethylene) to C₃H₆-C₃H₈ (propene – propane) mixtures. The fraction of heat radiated was found to lie between approximately 0.17 and 0.3.

3.2.7 Carter, 1991 [38]

The author describes the HSE jet flame thermal radiation model, MAJESTIC. A point source model is assumed and the thermal radiation, I (kW m⁻²) received at a distance, S (m), from the flame is given by:

$$I = \frac{fH_c\dot{m}\tau}{4\pi S^2 1000} \quad (58)$$

where:

- f = fraction of energy radiated;
- H_c = the heat of combustion (J kg⁻¹);
- \dot{m} = mass rate of fuel consumed (kg s⁻¹); and
- τ = the atmospheric transmissivity, which is taken from Clay et al. [20] (section 3.1.8) and is given by:

$$\tau = 1 - 0.0565 \ln(S) \quad (59)$$

3.2.8 Shell Research, 1991 [39]

The report details a programme of full scale horizontal jet fire experiments that were performed using a purpose built jet fire facility. The tests investigated natural gas and propane fires and considered both free burning flames and those impinging on obstacles. Discharge rates were in the range 2 to 12 kg s⁻¹.

The surface emissive power of the flames was calculated and found to range from 87 kW m⁻² to 203 kW m⁻² for methane, and from 112 kW m⁻² to 331 kW m⁻² for propane.

3.2.9 Cowley and Johnson, 1992 [40]

The report aims to describe the available knowledge at the time on oil and gas fires of relevance to offshore safety, including methods of prediction. It considers a number of different types of flame and investigates their shape as well as the emitted radiation.

The authors state that, for jet fires, radiation from soot dominates for most of the offshore fires considered. For sonic natural gas fires, however, the soot radiation can be quite small except at very large scale. The flame radiative characteristics are a function of the fuel type, the mass supply rate and the initial discharge momentum. The latter influences the amount of air entrainment.

The report states that there is a lot of information about the radiative characteristics of large-scale natural gas flames, but little is known about the radiative characteristics of large-scale flames from other hydrocarbons. Data from medium scale (7 to 20 megawatts)

jet flames which use a mixture of gas and liquid hydrocarbon as fuel seem to indicate that the radiation hazards could be worse than similar size natural gas or propane flames.

The authors discuss surface emissive powers, the fraction of heat radiated and the atmospheric transmissivity in relation to jet fires. For the SEPs, they note that there is considerable variation in the literature on the values to use. They state that the use of SEPs is debatable for jet fires as the radiation comes from deep within the flame and therefore the concept of a surface radiator is not valid.

The fraction of heat radiated has been studied at large-scale for natural gas jet fires, which indicate that it decreases with increasing jet exit velocity. The variation of the fraction of heat radiated with fuel type, however, has only been studied at laboratory scale.

For atmospheric transmissivity, the authors note that natural gas flames with release rates of a few kg per second do not produce large amounts of soot. The radiation from hot gases such as carbon dioxide and water is therefore significant. As this means the radiation is being emitted in wavelength bands close to the absorption bands of the gases in the atmosphere, more of the radiation is absorbed by the atmosphere than if there was a greater amount of soot present.

The authors discuss the predictive models that are available for jet flames and divide them into categories according to whether they are semi-empirical, integral models or field models (computational fluid dynamics models). Under the semi-empirical category, there is one single point source model, the API 521 model, several multiple point source models (e.g. WHAZAN and FLARESIM), and four “conical frustum” models i.e. solid flame models. It is stated that single point source models are inadequate for near field radiation predictions.

In the API point source model, a fraction of heat radiated of 0.2 is recommended for natural gas flames and 0.3 for all other hydrocarbons. The values are based on small scale experimental data. In the WHAZAN multiple point source model by Technica, the fraction of heat radiated is taken as 0.2 for all fuels and exit velocities.

Different equations are given for the flux from one source to an oriented receiving surface depending on whether the source is an isentropic or diffuse emitter. The model for an isentropic emitter assumes that the flame is transparent to radiation and therefore tends to over-predict the flux near to the flame. In the case of the diffuse emitter, however, it is assumed that the flame is opaque to radiation. In this case the flux is under-predicted close to the flame.

One solution to the problem of over- and under-predicting the flux is to assume that the source is a mixed emitter and to take the weighted average of each source. This approach has been used in the model FLARESIM where it is assumed that either there is a 50% contribution from each type of emitter to the flux, or it is assumed that the source is 60% an isentropic emitter and 40% a diffuse emitter. The method that gives the highest flux value is used.

FLARESIM assumes a fraction of heat radiated of 0.25 for subsonic releases and 0.1 for sonic releases. The model has been designed for natural gas flares.

For surface emitter models (i.e. solid flame models) it is stated that it is assumed that the surface emissive power is constant over the entire flame surface. The average SEP is calculated from the fraction of heat radiated and the idealised total surface area. The values of the SEP derived this way are highly model dependent and there is not a straightforward relationship between the effective radiant temperature derived from the SEP and the actual flame temperature. It is considered to be, however, slightly closer to reality than a point source model.

Most of the surface emitter models that are discussed are limited in their application as they only apply to small scale flames.

Most of the integral models discussed assume that a constant fraction of the energy produced locally by combustion is released as radiation. The values used range from 0.2 to 0.26. Only one of the models has been validated against large scale releases and this was for natural gas only.

3.2.10 Dutta et al., 1994 [41]

The paper reports the results of jet fire spray experiments of crude oil containing varying amounts of methane. The flame heights normalised by the external orifice diameter are shown together with normalised radiative heat fluxes and radiative heat loss fractions. The radiative fractions (or fraction of heat radiated) ranged from approximately 0.1 to 0.21. As the amount of methane increases, the radiative heat fraction decreases. If the methane to liquid ratio is kept constant, the fraction of heat radiated is shown to be independent of the heat release rate.

3.2.11 Johnson et al., 1994 [42]

The paper describes a natural gas jet fire model, including the thermal radiation, which is stated as being an extension and improvement of an earlier Shell model [9]. The flame shape and radiative properties are described by simple correlations which are based on measurements from 27 large-scale experiments.

The thermal radiation in natural gas jet fires comes from the combustion products and the soot. Compared to heavier hydrocarbons, there are relatively low concentrations of soot particles in a natural gas flame.

For the radiation section, the authors state that the fraction of heat radiated depends on the efficiency of combustion within the flame, the amount of energy lost by convection to entrained air, and the radiative properties of the combustion products. Soot radiates heat more efficiently than gases.

Account has to be taken of the size of the flame when transforming from the volume radiative emission of the real flame to the model surface radiative emission. If the release is horizontal, objects in the direction of the flame receive radiation from paths

approximately equal to the flame length, which is much greater than the flame width. Different values for the surface emissive power therefore need to be assigned to the ends and the side of the flame. This leads to a thermal flux equation of the form:

$$I = (F_{side}E_{side} + F_{end}E_{end})\tau \quad (60)$$

where:

- I = the thermal radiative flux (kW m^{-2});
- F_{side} = the view factor from the side of the flame;
- F_{end} = the view factor from the end of the flame;
- E_{side} = the SEP from the side of the flame (kW m^{-2});
- E_{end} = the SEP from the end of the flame (kW m^{-2}); and
- τ = the atmospheric transmissivity.

The authors state that the view factors are calculated using a “contour integration technique”, the details of which are not given but references are. For the atmospheric transmissivity, the equations of Wayne [30] (section 3.3.6) are used.

To calculate the SEP, an SEP from large scale flames with emitting path lengths long enough for the emission to be that of a black body, E_{∞} (kW m^{-2}), is first calculated:

$$E_{\infty} = \frac{f_{E_{\infty}}Q}{A} \quad (61)$$

where:

- $f_{E_{\infty}}$ = fraction of heat radiated for flames which emit black body radiation;
- Q = net heat released as combustion (kW); and
- A = total model flame surface area (m^2).

A grey gas approximation is used to calculate the different values of the SEP for the sides and ends of the flame, E (kW m^{-2}), reflecting the effects of varying path lengths through the flame:

$$E = (1 - e^{-kL})E_{\infty} \quad (62)$$

where:

- k = a grey gas absorption coefficient (m^{-1}); and
- L = a length scale representing the emitting path length (m).

The value of L was taken to be the predicted maximum width and frustum length for emission through the sides and ends of the flame respectively. Large scale experimental data was used to calculate the values of k and $f_{E\infty}$ by using Equations 61 and 62 in conjunction with Equation 60 and calculating values such that the predicted heat flux matched the measured heat flux. This led to a best fit value of k of 0.4 m^{-1} and a correlation for $f_{E\infty}$ of:

$$f_{E\infty} = 0.21e^{-0.00323u_j} + 0.14 \quad (63)$$

where u_j is the jet velocity (m s^{-1}). Note that this is very similar to the equation given in Chamberlain [9], with the only change being the constant added at the end.

3.2.12 Sekulin and Acton, 1995 [43]

The report documents the results of 43 large scale experiments of horizontal jet fires using mixtures of natural gas and butane. The concentrations varied between 100% natural gas and 100% butane. The flow rate was 2.5 kg s^{-1} in all experiments. An infra-red imaging system was used to provide a contour map of flame surface emissive power.

It was found that there was a trend for the surface emissive power to increase as the butane concentration increased when the spot SEP measurements were considered. The values ranged between approximately 100 kW m^{-2} to 200 kW m^{-2} . A similar trend was observed when considering the peak SEP, which reached maximums of approximately 250 kW m^{-2} .

3.2.13 Wade et al., 1995 [44]

The document reports the results of earlier laboratory scale experiments of spray jet fires of crude oil [42] mixed with varying amounts of methane (5% to 25% by mass). The work showed that two phase flow effects have a significant impact on the flame lengths and radiative fractions, which ranged from approximately 0.1 to 0.21.

The report details the results of 19 experiments with toluene that used the same experimental set up as the crude oil experiments. In this case, the toluene is mixed with 5% to 25% by mass of atomizing methane and 5% to 13% by mass of stabilising hydrogen. The radiative heat fractions were found to vary from less than 0.1 to approximately 0.45. The fraction of heat radiated was found to decrease as the methane to liquid ratio increased, as was the case in the crude oil experiments. This corresponds to a decrease in soot formation as the ratio of methane to toluene increases. As the hydrogen to liquid ratio increased, the fraction of heat radiated increased.

3.2.14 Selby and Burgan, 1998 [45]

A number of experiments are detailed in the report, including some on unconfined jet fires of stabilised light crude oil and mixtures of stabilised light crude oil and natural gas with release rates of 5 kg s^{-1} . It was found that the flames were luminous and generated large amounts of thick, black smoke. The maximum time-averaged values of flame surface emissive power ranged from 200 kW m^{-2} to 400 kW m^{-2} . The SEP increased with

increasing release pressure and increasing gas concentration. Total incident heat fluxes were higher for the mixed fuel tests than for the crude oil only tests.

3.2.15 Cumber, 2000 [46]

The field of view from a jet flame is discretised uniformly by the angle of rotation and the angle of incidence. The incident radiation intensity is assumed to be piecewise constant across the field of view of the receiver. The value of incident radiation intensity at the centroid of each element is taken to be representative of the whole element. To calculate the incident intensity over an element, rays are traced through the computational domain. These then form the input to a model that solves the equation of radiative heat transfer.

An improvement to the model is discussed which moves from a uniform ray distribution to one that is staggered across the angle of rotation. A further improvement proposes an adaptive algorithm that refines the mesh according to specified criteria.

3.2.16 Jo and Ahn, 2002 [47]

The authors consider the rupture of a natural gas pipeline. They calculate the release rate and some of the hazards associated with the pipeline failure. They also discuss the heat flux from any resultant fires. They consider a point source method, which assumes a point source located at the centre of the flame.

The discussion on heat flux relates to jet fires specifically. The heat flux, I (kW m^{-2}) is given by:

$$I = \frac{f\tau QH_c}{4\pi S^2} \quad (64)$$

where:

- f = the ratio of total heat radiated to total heat released from the fire;
- τ = the atmospheric transmissivity;
- Q = the gas release rate (kg s^{-1});
- H_c = the heat of combustion (J kg^{-1}); and
- S = the distance from the flame centre to the location of interest (m).

It is stated that the value of f cannot be calculated theoretically and must be estimated from data. For methane, a value of 0.2 is proposed. The atmospheric transmissivity is taken from an earlier version of the TNO Yellow Book and is quoted as:

$$\tau = 2.02(P_w R_H d)^{-0.09} \quad (65)$$

where:

- P_w = the partial water vapour pressure (N m^{-2});

- H = the relative humidity; and
- d = the distance from the pipeline failure point to the receiver (m).

It should be noted that the atmospheric transmissivity equation in the more recent version of the Yellow Book [25], does not explicitly include the relative humidity. The value of the partial water vapour pressure is instead taken at the relative humidity of interest.

3.2.17 Cleaver et al., 2003 [48]

The paper describes a numerical model for predicting all aspects of jet fires resulting from high pressure, sonic releases of natural gas. The radiation model partitions the field of view of a receiver into a number of elements with the incident radiation intensity assumed constant over each element. The value is taken at the centroid of the element and is calculated by tracing rays through the computational domain. The ray's orientation is defined by the centroid location on the unit hemisphere. The temperature and participating species concentrations for each ray in each finite-volume cell traversed are recorded and input to a statistical narrow band radiation model, which calculates the incident intensity. The incident flux integral is evaluated by summing the incident intensity distribution in a numerical integral approximation. The method is based on work by Lockwood and Shah [49] and Cumber [46, 50]. The paper details some of the modifications to the method that reduce the computational cost.

3.2.18 Lowesmith et al., 2007 [51]

The paper considers offshore hydrocarbon jet fires and the hazards that they pose. The standard equation for thermal radiation is given i.e. Equation 32, Page 21, which assumes a solid flame technique. The authors state that, at a distance of typically more than two flame lengths, a simplified point source technique can be used as an alternative. This does not require the flame shape to be defined.

The point source technique requires the calculation of the fraction of heat radiated, f :

$$f = \frac{EA}{1000Q} \quad (66)$$

where:

- E = the flame surface emissive power (kW m^{-2});
- A = the flame area (m^2); and
- Q = the net rate of heat released by combustion (MW).

The incident radiation, I (kW m^{-2}), is then:

$$I = \frac{1000\tau f \dot{m} H}{4\pi S^2} \quad (67)$$

where:

- τ = the atmospheric transmissivity
- \dot{m} = the mass flow rate (kg s^{-1});
- H = net calorific value (MJ kg^{-1}); and
- S = distance from the fire (m).

Higher values for the fraction of heat radiated are found in jet fires involving higher hydrocarbons. More soot is produced in these flames which generates higher emissions. The best fit value of fraction of heat radiated for crude oil experiments is 0.5, which is based on a comparison of radiative power with the net energy of combustion. However, when Lowesmith et al. investigate the effect of the size of 'water cut' with crude oil on the fraction of heat radiated, the data for releases with 0% water indicate that the value of fraction of heat radiated varies between 0.26 and 0.40. As the water content increases, the fraction of heat radiated decreases. This would seem to contradict the conclusion that the fraction of heat radiated for crude oil is 0.5 and would suggest that it is lower than this.

Kooi and Uijt de Haag [52] state that the upper end of the validation of the data in Lowesmith et al. was a release rate of 16 kg/s for crude oil.

For other substances, the best fit values of fraction of heat radiated are given as 0.13 for natural gas, 0.24 for propane and 0.32 for butane.

3.2.19 Gómez-Mares et al., 2009 [53]

This paper investigates the temperature distribution along a vertical jet axis. The paper presents experimental data for large (flame lengths up to 9 m) vertical sonic propane jet fires. It was found that the flames could generally be divided into three regions along the centreline according to temperature behaviour.

In the first region, the temperature increased with the axial position reaching values up to approximately 1800 K. This covers up to 40% of the jet flame length. The second region is from 40% to 70% of the flame length and it was found that the temperature profile showed a smooth variation. The average temperature remained close to 1800 K and maximum temperatures of up to 1900 K were observed. In the third region, the temperature began to decrease although higher temperatures were recorded at the tip of the flame than at the base.

3.2.20 Gómez-Mares et al., 2010 [54]

This paper reports the results of experimental tests of vertical propane jet fires. It was found that the heat radiated from the flame increases when there is two-phase flow. It is stated that this is due to the fact that the combustion is less efficient and that more soot is produced.

The paper discusses radiation in terms of the solid flame model i.e. Equation 54, page 29. It was found from the experiments that, as the flow rate increased, the amount of incident radiation at any location increased. A large amount of scatter was observed, however,

which they attribute to the turbulence phenomena as well as to flame size oscillation. It should be noted that the flow rates ranged from 0.09 kg s⁻¹ to 0.43 kg s⁻¹.

The observed incident radiation was used to calculate the surface emissive power of the jet flames, assuming that the flame is a cylinder. There was a significant amount of scatter in the data but the authors fit a trend line to the observations:

$$E = 22 + 10L \quad (68)$$

where:

- E is the surface emissive power (kW m⁻²); and
- L is the average flame length (m).

The authors note, however, that when the flame length is zero, the surface emissive power is non-zero which is not correct. They therefore propose an equation of the form:

$$E = aL^b \quad (69)$$

The values of the parameters a and b depend on which dataset is being used to derive the surface emissive power.

The average surface emissive power calculated from the observations of the vertical propane jet fires was between 50 and 100 kW m⁻².

The authors use the surface emissive power to calculate a fraction of heat radiated. They find that the average fraction of heat radiated is 0.07 with a standard deviation of 0.01. The low magnitude is explained by the fact that the jet fires in the study are sonic. As the exit velocity increases, the combustion quality increases and the radiant heat decreases.

3.2.21 Leroy and Duplantier, 2010 [55]

This paper uses the solid flame method to calculate the thermal radiation from a jet fire. The authors first calculate the surface emissive power, E (kW m⁻²) by relating it to the fraction of heat radiated, f :

$$E = \frac{f\dot{m}\Delta H_c}{A} \quad (70)$$

where:

- \dot{m} = the mass flow rate (kg s⁻¹);
- ΔH_c = total heat released (J kg⁻¹); and
- A = flame surface area (m²).

The fraction of heat radiated, f , is given by the equations in Cook et al. [56] (section 3.3.4) i.e.

$$f = \begin{cases} 0.21e^{-0.00323u_j} + 0.11 & MW < 21 \\ (0.21e^{-0.00323u_j} + 0.11) \left(\frac{MW}{21}\right)^{0.5} & 21 \leq MW \leq 60 \\ 1.69(0.21e^{-0.00323u_j} + 0.11) & MW > 60 \end{cases} \quad (71)$$

where:

- u_j = the jet velocity (m s⁻¹); and
- MW = the molecular weight of the fuel (kg mol⁻¹).

The model does not consider variations along the flame axis.

The radiative heat flux is given by the standard equation for a solid flame i.e.

$$I = E\tau F \quad (72)$$

where I is the heat flux (kW m⁻²), τ is the transmissivity of the atmosphere and F is the view factor.

3.2.22 Kozaoglu et al., 2011 [57]

The paper first discusses the findings from several other papers which showed that the fraction of heat radiated is dependent on the jet fuel, the jet exit velocity and the wind speed. As the hydrocarbon number increases, so does the fraction of heat radiated. This is generally due to an increase in the level of emissions which radiate more heat. Wind speed promotes a higher air entrainment rate which improves the quality of combustion and leads to lower fractions of radiated heat.

The paper goes on to discuss the influence of the jet velocity on the fraction of heat radiated. Experiments were conducted on sonic and subsonic propane jet fires leading to flame lengths of up to 8 m. The experimental results indicate that, as the mass flow rate increases, flame length increases which leads to a higher rate of convective heat transfer. Higher fuel exit velocity increases the air entrainment which creates stronger mixing and improved combustion. This leads to a less luminous flame with a lower rate of radiation. It was found that the fraction of heat radiated remained approximately constant but the convective heat transfer coefficient increases as the flow rate increases i.e. the transfer of heat through convection increases.

3.2.23 Hankinson and Lowesmith, 2012 [58]

This paper considers the calculation of the fraction of heat radiated from a jet flame. The authors quote the literature for an equation for the fraction of heat radiated, f , based on the single point source model:

$$f = \frac{I\pi S^2}{\dot{m}H_c\tau} \quad (73)$$

where:

- I = incident thermal radiation (kW m^{-2});
- S = distance from the single point to the receiver (m);
- \dot{m} = the mass flow rate (kg s^{-1});
- H_c = net calorific value (kJ kg^{-1}); and
- τ = the atmospheric transmissivity (kW m^{-2}).

The authors state that some of the literature has not included the atmospheric transmissivity, which leads to errors as the receiver moves further away from the fire. Other authors have used a different definition of S in the equation. In this case, the distance is from the receiver to a point perpendicular to the fire rather than to the single point source, which is normally considered to be at the centre of the fire.

The authors state that the point source approach is known to be inaccurate in the near field. This can become an issue if the value of f is being derived from experimental data, where the measurements of incident radiation were taken in the near field, rather than further away from the fire.

The authors describe a weighted multi-point source method as an alternative. They state that, as long as there are at least 20 point sources, the incident radiation is independent of the number of point sources. The point sources, w_j , are weighted such that:

$$w_j = jw_1 \quad \text{for } j = 1 \dots, n$$

$$w_j = \left[n - \frac{n-1}{N-(n+1)}(j-(n+1)) \right] w_1 \quad \text{for } j = n+1, \dots, N \quad (74)$$

$$\sum_{j=1}^N w_j = 1$$

where $1 \leq n \leq N$, N is the number of point sources. The authors use a value of $n = 0.75N$.

It is stated that the variation in weighting of the point sources along the flame trajectory and position of the peak used in the paper are not intended as final solutions, just as illustrations of the potential of the multi-point source method.

The incident radiation, I (kW m^{-2}), using the point source weightings, is given by:

$$I = \sum_{j=1}^N \bar{q}_j = \sum_{j=1}^N \frac{w_j f \dot{m} H_c \tau_j}{4\pi S_j^2} \cos \phi_j \quad (75)$$

where:

- τ_j = the transmissivity over the distance S_j from the j th point source to the receiver; and
- ϕ_j = the angle between the normal of the receiver and the line of sight to the j th point source.

The authors demonstrate good agreement with large scale data, in both the near-field and the far-field.

A method of comparing radiation models is presented, allowing the validity and general applicability of a fraction of heat radiated to be assessed in terms of its suitability for predicting near- and far-field radiation.

The authors conclude that the fraction of heat radiated is dependent on the method of derivation from experimental data. A value derived by one model may not be applicable to another model without adjustment. If incident radiation in the near-field is used to calculate the fraction of heat radiated, some correction will need to be applied to make it applicable in the far-field.

3.2.24 Kooi and Uijt de Haag, 2012 [52]

This report compares jet fire models in two risk assessment packages. In the first model, the JSFH-Cook model, the surface emissive power is derived by considering the total amount of heat radiated and the total surface area of the flame. If the molecular weight (M_w) of the fuel is less than 21 kg kmol^{-1} , then the fraction of heat radiated is taken from Chamberlain [9] (Equation 56, Page 30), which uses an equation that only depends on the expanded jet velocity. At higher molecular weights, the fraction of heat radiated, using the Chamberlain equation, is increased by a factor $(M_w/21)^{0.5}$, with an upper limit of 1.69 on the factor (as per Cook et al. [56], section 3.3.4).

The surface emissive power in the JSFH-Cook model is capped at 400 kW m^{-2} . If the SEP is capped, the fraction of heat radiated is decreased correspondingly.

The second model to be considered is the Barker LPG jet fire model. In this case, the SEP is determined by the temperature and the amount of soot in the flame. For propane, the SEP is capped at 230 kW m^{-2} , whereas, for butane, the cap is set at 255 kW m^{-2} . The fraction of heat radiated is calculated from the SEP, the surface area of the flame and the combustion power.

The third model is the Cracknell generic two-phase and liquid jet fire model. The fraction of heat radiated is calculated using a correlation linking the mass flow rate and the exit velocity (not given in the report). The correlation does not consider smoke obscuration. The fraction of heat radiated will therefore be conservative for high release rates. The SEP is derived from the total flame surface area, the total combustion power of the release, and the fraction of heat radiated.

The experimental data used for validation of the Cracknell model consisted of releases of butane/natural gas, propylene, kerosene/natural gas, two-phase propane, and two-phase butane. Release rates ranged from 0.05 to 22 kg s⁻¹.

All three models have been compared to data from crude oil jet fire experiments. In the first experiment, a maximum surface emissive power of 287 kW m⁻² was observed. The models predicted average SEPs of between 178 kW m⁻² and 258 kW m⁻². Note that the maximum SEP can vary significantly from the average SEP. In the second experiment, a maximum SEP of 203 kW m⁻² was observed and the model predictions of average SEP ranged from 176 kW m⁻² to 255 kW m⁻².

The results of the JFSH-Cook and Cracknell models indicate that the fraction of heat radiated decreases with increasing jet exit velocity. The results from the Barker and Cracknell models indicate that the fraction of heat radiated also decreases with increasing discharge rate.

The fraction of heat radiated calculated by the three models has been compared to a range of experimental data. The data consists of butane, butane and natural gas mixtures, and crude oil. The models have been run assuming a butane release at 66 m s⁻¹ but varying the release rate from less than 10 kg s⁻¹ up to approximately 10,000 kg s⁻¹.

The results from the JFSH-Cook model for show that the fraction of heat remains constant at approximately 0.47 until the release rate reaches approximately 300 kg s⁻¹, at which point it steadily decreases, reaching a minimum value of approximately 0.28 at 10,000 kg s⁻¹. The Barker model starts at approximately 0.37, reduces steadily to a value of approximately 0.12 by about 100 kg s⁻¹ and then remains constant. The Cracknell model starts at the same value as the Barker model but decreases steadily, reaching a minimum value of approximately 0.18 by 10,000 kg s⁻¹.

The data used for the comparison shows a wide variety of scatter and the maximum release rate is approximately 30 kg s⁻¹. The butane data shows a general downward trend in the fraction of heat radiated as the release rate increases from approximately 0.45 at 1 kg s⁻¹ to less than 0.2 at approximately 30 kg s⁻¹. The butane and natural gas mixture data appears to be for a single release rate and the fraction of heat varies from 0.1 to 0.39. The crude oil results are over a narrow range of release rates and vary from approximately 0.35 to 0.67. No real trend can be inferred from the data.

The authors state that the Cracknell model is expected to give the most reliable results for the fraction of heat radiated for the three models investigated. This is due to the fraction of heat radiated being derived from a relatively sophisticated physical argument in combination with experimental data. The validation also includes two phase mixtures. In particular, the predictions are considered to be the most accurate for large jet fires.

The authors discuss the physical mechanisms for heat radiation from flames. Two types of energy are produced. The first is convective energy, which is the heating of the combustion products and the entrained air, and the second is heat radiation. The heat

radiation is predominantly produced by soot in the flame. Soot is both a good emitter and a good absorber of heat radiation and the influence of the soot depends on whether the flame is optically thick or thin:

- Optically thin flames – In the optically thin regime, an increase of soot produces more radiation while absorption of radiation remains low. In this regime, a larger amount of soot results in a higher amount of heat radiation received by an observer outside the flame.
- Optically thick flames – In the optically thick regime, soot in the outer regions of the flame absorbs the radiation produced in the inner regions of the flame, i.e. the inner region of the flame is shielded. As a consequence, only the radiation produced in the outer regions of the flame is relevant for observers outside the flame. In this regime, the received heat radiation depends on the size of the flame and is not very sensitive to the specific amount of soot.

The amount of soot in a flame is determined by the type of fuel and the quality of the mixing with air. Fuels with higher carbon numbers produce more soot than fuels with low carbon numbers. Good mixing reduces the amount of soot. Release rate and jet exit velocity have the greatest effect on the mixing rate.

For release rates above 25 kg s^{-1} , the authors consider the flame to be optically thick i.e. soot in the outer regions of the flame absorbs the radiation produced in the inner regions of the flame meaning that the inner region of the flame is shielded. The received heat radiation depends on the size of the flame and is not very sensitive to the specific amount of soot.

The authors quote work by Barnwell and Marshall [59] which reports the fraction of heat radiated as a function of jet exit velocity and shows the effect of hydrocarbon type. For propane, the fraction of heat radiated diminishes from approximately 0.37 at 0 m s^{-1} to 0.15 at an exit velocity of 60 m s^{-1} . For methane, the reduction is lower but it is still shown to decrease from approximately 0.20 for a velocity of 5 m s^{-1} to just below 0.15 at an exit velocity of 70 m s^{-1} .

The fraction of heat radiated is initially higher for propane than for methane, but it decreases more rapidly with increasing jet velocity. The initially higher value of the fraction of heat radiated for propane is due to more soot being produced when it burns than methane. As the jet velocity increases, the mixing of the fuel with the air increases, leading to lower amounts of soot and hence a lower fraction of heat radiated.

3.2.25 Palacios et al., 2012 [60]

This paper uses the results of large scale propane jet fire experiments to show that the jet fire can be divided into three zones, with different average temperatures associated with each of them. The temperatures range from 968 K to 1370 K, with average values of between 1200 K and 1260 K.

Average surface emissive powers were calculated from the experiments for the three zones. These ranged from 57.8 kW m⁻² to 80.7 kW m⁻², with an average value of 69.5 kW m⁻².

The solid flame model was used to estimate the intensity of thermal radiation received at specific targets. Two approaches were used: the first assumed a single zone and used the average value for surface emissive power; the second broke the jet fire into three regions and used the surface emissive power appropriate to each region. In both cases, the atmospheric transmissivity, τ , was given by:

$$\tau = 0.79 \left[\frac{100}{R_H} \right]^{1/16} \left[\frac{30.5}{S} \right]^{1/16} \quad (76)$$

where:

- R_H = relative humidity of the atmosphere (%); and
- S = distance from the flame surface to the exposed target (m).

3.3 Fireballs and jet fires

3.3.1 Croce and Mudan, 1986 [22]

The paper considers the thermal radiation hazards from pool fires, jet fires, fireballs and vapour cloud fires. It looks at different models for calculating the radiation and starts with the point source model. The total amount of heat radiated from the fire is assumed to radiate uniformly in all directions. If a spherical surface is assumed, the incident flux, I (kW m⁻²) is given by:

$$I = \frac{f \dot{m} \Delta H_c}{4\pi L^2} \quad (77)$$

where:

- f = the fraction of heat radiated;
- \dot{m} = the burning rate (kg s⁻¹);
- ΔH_c = the heat of combustion (J kg⁻¹); and
- L = the distance from the fire to the target (m).

The authors state that the value of the fraction of heat radiated can vary from about 0.1 for LNG to about 0.6 for gasoline. In general, the value is small for small fires, increases to a fairly constant value as the fire increases and produces more radiating soot, and then decreases as the fire gets even larger. At this point, the fire produces so much soot that it shields the flame, preventing all the heat from radiating outwards.

The second technique discussed is the solid flame model, which produces more accurate results, particularly close to the fire. The remainder of the paper concentrates on the use of this technique for the different types of fire.

The surface emissive power, E (kW m⁻²) of a fire is given by:

$$E = \varepsilon \sigma T_f^4 \quad (78)$$

where:

- ε = flame emissivity (kW m⁻²);
- σ = the Stefan-Boltzmann constant (5.670373×10^{-11} kW m⁻² K⁻⁴); and
- T_f = temperature at the surface of the fireball (K).

The flame emissivity, ε , is given as a function of a path length (between the fire and the receiver), S (m), and an extinction coefficient parameter, k_m (m⁻¹):

$$\varepsilon = 1 - \exp(-k_m S) \quad (79)$$

Values of k_m generally lie in the range 0.5 m⁻¹ to 5 m⁻¹, implying that, for large fires where S can be many metres, the value of the emissivity approaches 1.

It is stated that turbulent jet fires are generally relatively well mixed compared to other types of fire. For large jets this can mean that less soot is produced and that the jets have higher emissive powers. A table of jet flame temperatures and surface emissive powers that they state are “based upon Schmidt temperature measurements” is provided. The information is reproduced in Table 1.

Table 1 Flame temperatures and surface emissive powers from Croce and Mudan [22]

Hydrocarbon	Flame temperature (K)	Emissive power (kW m ⁻²)
Methane	1500	290
Ethane	1590	360
Ethylene	1720	500
Propane	1560	340
n-butane	1610	380
Propylene	1490	280
Butylene	1410	220

For fireballs, the authors argue that, as the fireball is well mixed, the same emissive powers that apply to jet flames can be used.

3.3.2 Crocker and Napier, 1988 [61]

The paper investigates fires and explosions as a result of LPG releases and aims to model the thermal radiation and overpressures. For jet fires with no wind, the Stefan-Boltzmann equation is used in conjunction with an appropriate view factor and atmospheric transmissivity i.e.

$$I = F\varepsilon\sigma T_f^4\tau \quad (80)$$

where:

- I = the thermal radiation (W m^{-2});
- F = the view factor;
- ε = flame emissivity (W m^{-2});
- σ = the Stefan-Boltzmann constant ($5.670373 \times 10^{-8} \text{ W m}^{-2} \text{ K}^{-4}$);
- T_f = radiation temperature (K); and
- τ = atmospheric transmissivity.

The authors have also considered jet fires in a windy atmosphere. In this case, they use a point source model to estimate the radiation, I (W m^{-2}), using the equation:

$$I = \frac{fQ\cos\beta}{4\pi S^2} \quad (81)$$

where:

- f = fraction of heat released as radiation;
- Q = rate of heat release (kJ s^{-1});
- β = angle between normal and line joining point source and target flame emissivity; and
- S = distance between point source and target (m).

Variations of Equation 81 are given to consider specific target locations.

The authors also consider a multiple point source model for a jet fire. In this case, the total intensity of radiation, I (W m^{-2}), is given by:

$$I = \int_A \frac{\varepsilon\sigma T_f^4 \cos\beta}{4\pi S^2} dA \quad (82)$$

where:

- ε = flame emissivity (W m^{-2});

- σ = the Stefan-Boltzmann constant ($5.670373 \times 10^{-8} \text{ W m}^{-2} \text{ K}^{-4}$);
- T_f = flame temperature (K);
- β = angle between normal and line joining point source and target flame emissivity;
- S = distance between point source and target (m); and
- dA = differential area of the flame (m^2).

Correlations are used to derive the geometry of the flame, and hence the thermal radiation.

The authors go on to consider fireballs. In the first instance, a ground level fireball is considered which is instantly at its maximum diameter and remains at this size for its duration. The radiation, I (W m^{-2}), can be calculated using:

$$I = \varepsilon \sigma T_f^4 \frac{D^2 x}{4S^3} \quad (83)$$

where:

- D = fireball diameter (m);
- x = the horizontal position of the target;
- S = position from the point source to the target (m); and
- The other parameters are as in the previous equations.

A dynamic fireball model is also considered. In this instance the radiation, I (W m^{-2}), is calculated according to:

$$I = \varepsilon \sigma T_f^4 F(t) \quad (84)$$

where:

- t = time (s);
- $F(t)$ = the view factor, which varies by time as the fireball rises and grows; and
- The remaining parameters are as in the previous equations.

Equation 84 is equivalent to Equation 83, noting that the fractional term in Equation 83 is the view factor. In both cases, the atmospheric transmissivity has not been included.

3.3.3 Bagster and Pitblado, 1989 [62]

The first section of this paper considers pool fires and provides equations for burning rates, mass burning rate, total heat production, flame height, flame tilt, and flame drag.

The next section provides a discussion on the emissive power of flames (E , $W m^{-2}$), with the general equation for all types of flame given as:

$$E = \varepsilon\sigma T_f^4 \quad (85)$$

where:

- ε = flame emissivity ($kW m^{-2}$);
- σ = the Stefan-Boltzmann constant ($5.670373 \times 10^{-11} kW m^{-2} K^{-4}$); and
- T_f = temperature at the surface of the flame (K).

An alternative method for estimating emissive power is based on the calculation of the total heat production, Q_R (kW):

$$E = \frac{Q_R}{A} \quad (86)$$

where A is the flame surface area (m^2).

The authors consider the emissive power of large liquid hydrocarbon fuel fires (with a carbon to hydrogen ratio of greater than 0.3), in particular kerosene and gasoline fires on water. Such fires are largely obscured by black smoke which absorbs a large amount of radiation and results in little emission. At times, pulses of radiation are emitted through openings in the smoke layer, however. These two regions of the fire have very different emissive powers and the authors propose that they can be combined if the fraction of the time that the surface area is covered in black smoke is known.

The radiation is first discussed in terms of a point source model. In this case, the radiant intensity, I ($kW m^{-2}$), at any distance, S (m) is given by:

$$I = \frac{Q_R}{4\pi S^2} \quad (87)$$

The standard equation for a solid flame model (Equation 32, Page 21) is also quoted. The authors initially quote an equation given by Lihou and Maund [14] for the atmospheric transmissivity (Equation 30, Page 19). They state that it is related to visibility and does not explicitly include absorption, which has a greater effect on atmospheric transmissivity. As an alternative, they quote an equation from an earlier version of the "Yellow Book" [25], where the transmissivity, τ , is related to the actual water partial pressure, P_w (Pa), given by:

$$\tau = 1.382 - 0.135 \log_{10}(P_w S) \quad (88)$$

They state that the equation was revised to that in the current version of the "Yellow Book":

$$\tau = 2.02(P_w S)^{-0.09} \quad (89)$$

3.3.4 Cook et al., 1990 [56]

This paper describes two jet fire models and one BLEVE model. The geometry part of the BLEVE model is HSE's FBALL model [5]. Equations are given for the calculation of surface emissive power, E (kW m^{-2}) for jet fires and BLEVEs. The equation for a jet fire is given by:

$$E = \frac{f\dot{m}H_c \times 10^{-3}}{A} \quad (90)$$

where:

- f = the fraction of heat radiated;
- \dot{m} = the mass discharge rate (kg s^{-1});
- H_c = the heat of combustion (J kg^{-1}); and
- A = the surface area of the flame (m^2).

The fraction of heat radiated is based on the equation given by Chamberlain [9] but with an additional factor included to account for two-phase and liquid jets:

$$f = [0.21e^{-0.00323u_j} + 0.11]F(MW) \quad (91)$$

where $F(MW)$ is a function of the molecular weight to account for the observed variation of f with the molecular weight (MW (kg kmol^{-1})) of the gas being released and is given by:

$$F(MW) = \begin{matrix} 1 & MW < 21 \\ (MW/21)^{1/2} & 21 < MW < 60 \\ 1.69 & MW > 60 \end{matrix} \quad (92)$$

The surface emissive power, E (kW m^{-2}), of a BLEVE is given by:

$$E = \frac{fmH_c \times 10^{-3}}{4\pi r^2 t} \quad (93)$$

where:

- f = the fraction of heat radiated;
- m = the combustible mass (kg);
- H_c = the heat of combustion (J kg^{-1});
- r = the fireball radius (m); and
- t = the fireball duration (s).

The fraction of heat radiated is that given by Roberts [4]:

$$f = 0.00325P^{0.32} \quad (94)$$

where P is the saturated vapour pressure of the fuel (Pa).

Note that the change of units, from MPa in Roberts to Pa here, has modified the constant multiplier in the equation.

The solid flame method is used to calculate the radiation i.e. the radiation, I (kW m⁻²), incident at a point is given by:

$$I = E\tau F \quad (95)$$

where:

- E is the surface emissive power (kW m⁻²);
- τ is the atmospheric transmissivity; and
- F is the view factor.

The atmospheric transmissivity is stated as being taken from a figure in Raj [63] and is given by:

$$\tau = 1.389 - 0.135 \log_{10}(P_w S) \quad (96)$$

where:

- P_w = the partial pressure of water vapour in the air (Pa); and
- S = the distance from the flame to the receiver (m).

It should be noted that the transmissivity equation cannot be found directly in Raj, but appears to have been calculated based on a graph of transmissivity against path length.

3.3.5 Satyanarayana et al., 1991 [16]

The paper lists four methods of calculating the atmospheric transmissivity from the wider literature. The first is said to come from Lihou and Maund [14], with the transmissivity, τ , being given by:

$$\tau = \exp\left(\frac{-KS}{1000}\right) \quad (97)$$

where:

- K = a visibility factor, 0.7 in Lihou and Maund; and
- S = the distance between the target and the centre of the fireball (m).

An alternative equation is quoted as being from HSE. This is the equation currently used by HSE in some of their jet fire models [8]. HSE does not use it for the fireball model, although that is the subject of the Satyanarayana paper:

$$\tau = 1 - 0.058 \ln(S) \quad (98)$$

The remaining two methods are quoted as being from TNO, although the reference given is to Bagster and Pitblado [62]. The equations are given as:

$$\tau = 1.382 - 0.135 \log_{10}(P_w S) - 0.09 \quad (99)$$

and a modified version:

$$\tau = 2.02(P_w S) \quad (100)$$

where:

- P_w = partial water vapour pressure (Pa); and
- S = distance from the target to the centre of the fireball (m).

It should be noted that Equation 99 could not be found in the latest version of the “Yellow Book” from TNO [25] and, differed from Bagster and Pitblado by including -0.09 at the end. In addition, Equation 100 appears to be missing an exponent of -0.09 on the quantity within the brackets (it is quoted later in the paper correctly).

3.3.6 Wayne, 1991 [30]

The paper reviews methods for calculating atmospheric transmissivity from the wider literature, including the spectral transmissivity methods of Wyatt et al. [64] and Stull et al. [65]. In their papers, tables of the transmissivity of water vapour and carbon dioxide as a function of frequency and the pressure \times the path length of the absorbing species were compiled. The transmissivity, τ , could then be calculated for any path through any mixture of carbon dioxide and water according to:

$$\tau = \tau_{H_2O} \tau_{CO_2} \quad (101)$$

According to Wayne, there is an intrinsic dependency on the atmospheric temperature that means that, at temperatures either much lower or higher than 300 K, the tables may be inaccurate. Within the range of atmospheric temperatures of interest, however, the tables should be acceptable.

From the tables of Stull et al. [65], an expression can be derived for the amount of carbon dioxide in the absorbing path using the amount at 273 K:

$$CO_2 = L \times 100 \times P \times 335 \times 10^{-6} \times \frac{273}{T} \quad (102)$$

where:

- CO_2 = amount of carbon dioxide in the path (atm cm);
- L = the path length (m);
- P = atmospheric pressure (atm); and
- T = atmospheric temperature (K).

Similarly, the amount of water vapour can be expressed as:

$$H_2O = L \times S_{mm} \times R_H \times \frac{2.88651 \times 10^{-2}}{T} \quad (103)$$

where:

- H_2O = amount of water vapour (precipitable cm);
- L = the path length (m);
- T = atmospheric temperature (K);
- S_{mm} = saturated water vapour pressure (mm Hg) at the atmospheric temperature, T ; and
- R_H = relative humidity.

Note the 10^{-2} term on the right hand side of the equation. This is later revised in the paper to 10^2 which is more appropriate, given the change in units from metres to centimetres. This is reflected in the equations quoted subsequently.

Spectral transmissivities can be obtained for 188 windows of absorption for water and carbon dioxide and used to construct the transmissivity curve. The total or average transmissivity of the atmospheric path “is obtained by comparing the integrated intensity of the transmitted spectrum with the integrated intensity of the emitted spectrum”.

Wayne concludes that none of the methods are suited to “the rapid calculation of large numbers of transmissivities”, and instead proposes a revised method, based on the spectral transmissivity method, that is suitable for the temperature range 253-313 K. The author states that it is likely to be less accurate at temperatures below 273 K than at the higher temperature range.

The author states that the proposed method is applicable only “to sources that can be assumed to emit predominantly continuum radiation (as opposed to line or banded radiation), and the assumed source spectrum should not vary rapidly compared with the resolution of the wavelength grid”. It is further stated that “radiation from the hot gaseous products of combustion forms an important part of the total radiative output of LNG pool fires below 10 m in diameter and of high-velocity jet fires.” The method is considered unsuitable for these types of fire.

It has been assumed that the fire emits radiation as a black or grey body at 1500 K. It is stated that the calculated transmissivities do not vary rapidly over a range of temperatures of a few hundred K. It is also assumed that there is no dependence of the intrinsic absorption behaviour of carbon dioxide and water on atmospheric temperature.

The amount of carbon dioxide in the path, $X(CO_2)$ (m), is given by:

$$X(CO_2) = \frac{273L}{T} \quad (104)$$

where:

- L = path length (m); and
- T = atmospheric temperature (K).

The amount of water vapour in the path, $X(H_2O)$ (μm), is given by:

$$X(H_2O) = \frac{2.88651 \times 10^2 R_H L S_{mm}}{T} \quad (105)$$

where:

- R_H = fractional relative humidity; and
- S_{mm} = saturated water vapour pressure in mm of mercury, at the atmospheric temperature, T (K).

A calculation was performed using the tables of Wyatt et al. [64], which allowed a base set of 70 atmospheric transmissivities to be generated at a temperature of 297 K and for a range of relative humidities. From this, a polynomial approximation was applied to derive a correlation. The resultant equation for the atmospheric transmissivity, τ , is:

$$\begin{aligned} \tau = & 1.006 - 0.01171 \log_{10}(X(H_2O)) - 0.02368 \left(\log_{10}(X(H_2O)) \right)^2 \\ & - 0.03188 \log_{10}(X(CO_2)) \\ & + 0.001164 \left(\log_{10}(X(CO_2)) \right)^2 \end{aligned} \quad (106)$$

If the relative humidity is zero, then $X(H_2O)$ should be set to 1.

Equation 106 can be used for any relative humidity, for path lengths between 10 and 1000 m and through atmospheres at temperatures between 253 and 303 K. It is subject to the restriction of a fire temperature of 1500 K although, as previously stated, the transmissivity does not vary significantly within a few hundred K of this temperature. It is applicable to black or grey radiators.

3.3.7 Kay, 1994 [66]

This book details radiation calculations for pool fires, jet fires and fireballs. The solid flame technique is used to calculate the thermal radiation and a number of worked examples are given for pool fires and fireballs.

The flame surface emissive power is given by the Stefan-Boltzmann equation, with the calculated value adjusted to take account of the flame emissivity (i.e. Equation 85, Page 49). The authors also consider the absorptivity of the receiving target.

The atmospheric transmissivity is based on the work of Simpson [18]. The authors note that the amount of radiation absorbed by the atmosphere does not vary greatly with flame temperatures between 1100 K and 1500 K. They therefore use an approximation based on a single parameter, the distance to the receiving target. It appears that the transmissivity is read from a graph, as no equation is given.

Appendix VII of the book contains tables of surface emissive powers and flame temperatures for a range of substances. Some of these are for pool fires and some are taken from information on jet fires. The jet fire information and some of the pool fire data is taken from Croce and Mudan [22] and has been quoted in Section 3.3.

3.3.8 Crawley et al., 2003 [67]

This paper includes a comparison of surface emissive powers in the literature and states that they range from over 1000 kW m⁻² to less than 50 kW m⁻². They state that it is important to understand the fuel source and the flame structure and that jet or premixed flames are well aerated and burn more cleanly than pool fires. They discuss a series of tests conducted by BP ("Hot stuff: an introduction to fire hazards") which quotes flame temperatures and maximum heat transfer fluxes. These indicate that the surface emissive power cannot exceed 350 kW m⁻² and that the peak temperatures were of the order of 1573 K.

The authors note that the nature of the flame i.e. its temperature and emissivity are important. Methane flames produce very little soot and are therefore grey body radiators. This means that they burn with flame colours approaching the white end of the spectrum and with temperatures of over 1700 K. Heavy hydrocarbons, in contrast, produce carbon. If there is sufficient carbon, the flame can act as a black body and the emissivity can approach one. Actively aerated flames at or nearest to the jet will be optically thin. In this case, the theoretical maximum SEP is 350 kW m⁻² but the true value is likely to be nearer 275 kW m⁻².

The authors determine that the SEP for the fireball from the Piper Alpha disaster could not exceed 330 kW m⁻² and that, due to incomplete combustion, the value is likely to be nearer 225 kW m⁻².

For oil fires, the theoretical maximum SEP lies in the range 350 kW m⁻² to 400 kW m⁻² but true values are likely to be lower. Methane flames approach translucent and give SEPs which would not exceed 75 kW m⁻². Ethane can produce smoky flames leading to a maximum SEP of 350 kW m⁻².

3.3.9 TNO, 2005 [25]

Chapter 6 of the “Yellow Book” considers the heat flux from fires. The surface emissive power, E (W m^{-2}) for a “grey” radiator is given by:

$$E = \varepsilon\sigma(T_f^4 - T_a^4) \quad (107)$$

where:

- ε = flame emissivity (W m^{-2});
- σ = the Stefan-Boltzmann constant ($5.670373 \times 10^{-8} \text{ W m}^{-2} \text{ K}^{-4}$);
- T_f = temperature of the radiator surface of the flame (K); and
- T_a = atmospheric temperature (K).

If $\varepsilon = 1$, the flame is considered to be a “black radiator”. Equation 107 provides the theoretical maximum value for the SEP but can be difficult to derive as the flame temperature is generally not known and can vary across the dimensions of the flame.

An alternative method is to calculate a theoretical value of the SEP, E_{theor} , using the combustion energy per second, Q (W) and the flame surface area, A (m^2):

$$E_{theor} = Q/A \quad (108)$$

The combustion energy per second can be given by:

$$Q = \dot{m}H_c \quad (109)$$

where:

- \dot{m} = mass flow rate (kg s^{-1}); and
- H_c = heat of combustion (J kg^{-1}).

A maximum value for the SEP, E_{max} , can be calculated from the theoretical value, assuming a value for the fraction of heat radiated from the flame surface, f :

$$E_{max} = fE_{theor} \quad (110)$$

The actual value of SEP, E_{act} is less than the maximum value due to the absorption capabilities of soot and smoke and can be given by:

$$E_{act} = E_{max}(1 - \zeta) + E_{soot}\zeta \quad (111)$$

where ζ is the fraction of the surface of the flame covered by soot.

The heat flux, I (W m^{-2}), is given by:

$$I = E_{act} F \tau \quad (112)$$

where:

- F = the view factor; and
- τ = atmospheric transmissivity.

The atmospheric transmissivity is given by 1 minus the absorption factors for water and carbon dioxide, α_w and α_c i.e.

$$\tau = 1 - \alpha_w - \alpha_c \quad (113)$$

It can be difficult to calculate the absorption factors and an alternative simplified equation is given as:

$$\tau = 2.02(P_w S)^{-0.09} \quad (114)$$

where:

- P_w = partial water vapour pressure of water in air at a relative humidity, RH (Pa); and
- S = distance from the surface area of the flame to the object (m).

The equation can be used for varying values of relative humidity as it has been found that the values of τ are relatively insensitive to the relative humidity. It is stated that the formula can only be used when the value of $p_w x$ lies between 10^4 and 10^5 N m⁻¹.

The equation is referenced as being by Bagster and Pitblado [62] but they, in turn, refer back to an earlier version of the “Yellow Book”. Other references have also been investigated but the origin of the equation has not been traced.

The fraction of heat radiated, f , for a fireball is quoted as being from Roberts [4] and is given as:

$$f = 0.00325P^{0.32} \quad (115)$$

where P is the saturated vapour pressure before release (Pa). Note the change in the units when compared to Roberts (Equation 26, Page 18) which affects the constant multiplier.

For jet fires, the fraction of heat radiated is calculated using Equation 56 from Chamberlain [9] (Page 30).

3.3.10 Lehr et al., 2008 [68]

This paper describes the model used in the Areal Locations of Hazardous Atmospheres (ALOHA) model to calculate the thermal radiation that a receiver is exposed to from a pool fire, BLEVE, flammable or explosive vapour cloud, and a flare.

ALOHA uses a surface emissive power in its BLEVE radiation calculations that is 350 kW m⁻² multiplied by the ratio of the heat of combustion of the chemical divided by the heat of combustion of propane. The model assumes that radiation levels are fixed at a constant level during the last two-thirds of the fireball's duration, in contrast to experimental data which indicates that the peak radiation reduces over this time period.

The equation for atmospheric transmissivity, τ , is taken from Cook et al. [56] and is given by:

$$\tau = 1.382 - 0.135 \log_{10}(P_w S) \quad (116)$$

where:

- P_w = the partial pressure of water vapour in the air (Pa); and
- S = the distance between the target and the flame (m).

Note that there is a discrepancy between the equation reported by Lehr et al. and the one given by Cook et al. [56]. The first term on the right hand side of Equation 116 is given as 1.389 in Cook et al.

The standard equation for the view factor from a sphere is given, noting that ALOHA assumes that the fireball does not rise from the ground.

The incident radiation, I (kW m⁻²) is calculated assuming a solid flame model i.e.:

$$I = E\tau F \quad (117)$$

where E is the surface emissive power (kW m⁻²) and F is the view factor.

The jet fire model in ALOHA uses the equations from Chamberlain [9], including the equation for the fraction of heat radiated from the flame's surface (Equation 56, Page 30). Each part of the flame surface is assumed to radiate the same amount of energy. The total amount of energy emitted is determined by the heat of combustion multiplied by the mass release rate and the fraction of heat radiated.

3.3.11 Lowesmith and Hankinson, 2013 [69]

The paper describes two large scale pipeline experiments using natural gas and a natural gas/hydrogen mixture. The incident thermal radiation was calculated across a distance of up to 200 m. Using a multi-point source technique, the fraction of heat radiated with time was calculated. This was shown to range from approximately 0.25 to 0.4 for the mixture and from 0.2 to 0.3 for the natural gas experiment.

In a further report seen by the author that is not in the public domain, flame surface emissive powers of over 859 kW m⁻² were observed.

3.3.12 Cleaver and Halford, 2015 [70]

The paper describes a model for the initial stages of a release of natural gas from a transmission pipeline. It considers the crater, the initial jet fire (the “stalk”) and the fireball (the “cap”). The model uses a correlation for the fraction of heat radiated for the stalk, which is based on predictions of the PIPESAFE [71] model once a stable jet fire is established. The correlation is:

$$f = \min(0.5, \dot{m}_0^{-1/6})(0.28 + 0.31e^{-0.2U_{10}}) \quad (118)$$

where:

- f = the fraction of heat radiated;
- \dot{m} = the mass flow rate (kg s^{-1}); and
- U_{10} = the wind speed at an elevation of 10 m (m s^{-1}).

Lower and upper limits of 0.07 and 0.35 respectively are imposed for f .

For the cap, a representative peak temperature, T^C (K) is calculated from the bulk temperature, T (K):

$$T^C = K(T - T_\infty) + T_\infty \quad (119)$$

where T_∞ (K) is the atmospheric temperature and $K \geq 1$ is a constant.

The assumption of Moorhouse and Pritchard [17] that a greater fraction of heat is radiated from fireballs than jet fires is used to propose that the fraction of heat radiated is 60% higher for fireballs than for jet fires i.e. Equation 118 is multiplied by 1.6. The value of K in Equation 119 is chosen so that this fraction of heat is radiated by the cap.

Flame temperatures are calculated in the model for the jet fire element. HSE have been provided with some output from the model which indicates that the maximum flame temperature from the “stalk” is approximately 850 to 900 K. These temperatures would imply SEP values of between 30 and 40 kW m^{-2} .

3.4 Discussion

There are two main methods discussed within the literature for calculating the radiation from a fire. The first of these is the point source method, or a multi-point source method, whilst the second is the solid flame method. The latter considers the geometry of the flame, whilst the former uses assumptions that mean the geometry of the flame does not need to be considered. It is recognised that the point source method is less accurate than the solid flame method in the near field. The solid flame method has generally been used for fireballs, where the geometry is relatively simple, assuming a spherical fireball. For jet fires, both methods have been used.

In order to use the solid flame method, the surface emissive power of the fire, the transmissivity of the atmosphere and the view factor from the flame to the object/person are required. The point source, or the multiple point source method, requires knowledge of the fraction of heat radiated.

It is useful to split the discussion into two sections, one considering fireballs and one considering jet fires. Historically, within MISHAP, the radiation from the two types of fire has been calculated using different equations. The discussion will consider whether or not this should still be the case.

In addition, the values for the surface emissive power from the literature are summarised in Table 2. Table 3 reports the values for the fraction of heat radiated.

Table 2 Summary of surface emissive powers (E) from the literature

Source	Applicable types of fire	Surface emissive power (kW m⁻³)	Comments
Chaplin [8]	Fireballs	200 for fireballs \geq 125 te 270 for fireballs $<$ 125 te	For all substances. Origin unknown.
Chaplin [8]	Jet fires	256 for pipeline ruptures 300 for holes in pipelines	For natural gas fires only. Origin unknown.
Chamberlain [9]	Jet fires	191 to 254	Calculated from experimental measurements of natural gas fires.
Moorhouse and Pritchard [17]	Fireballs	Min 150 Max 300 $E = 235P^{0.39}$	Assumed range for pure vapour fireballs based on the small scale experiments of Hasegawa and Sato [12]. Correlation applicable for fuel masses up to 6.2 kg.
Johnson and Pritchard [21]	Fireballs	Top of fireball up to 500 Remainder 250 to 350 Mean across fireball 306 to 368	Results of 2 tonne propane and butane vessel experiments.
Prugh [23]	Fireballs	89 to 200	Based on flame temperatures assumed from flame colour. Fireballs assumed to be at the upper end of the range.

Source	Applicable types of fire	Surface emissive power (kW m ⁻³)	Comments
Roberts et al. [31]	Fireballs	Mean 240 to 400 Max 480 to 650	Results of 2 tonne propane vessel experiments.
Cook et al. [36]	Jet fires	Mean 239	Based on natural gas field scale experiments. The SEP varies along the flame length. Maximum value occurs at the centre.
Shell Research [39]	Jet fires	87 to 203 for methane 112 to 331 for propane	Based on large scale experimental data.
Sekulin and Acton [43]	Jet fires	100 to 200 for natural gas/butane mixtures	The SEP was found to increase as the concentration of butane increased.
Selby and Burgan [45]	Jet fires	200 to 400	Based on experimental data from unconfined jet fires of crude oil and crude oil/natural gas mixtures.
Gómez-Mares et al. [54]	Jet fires	50 to 100 $E = 22 + 10L$ where L is the average flame length (m)	Calculated using observed incident radiation from vertical sonic propane jet fires.
Kooi and Uijt de Haag [52]	Jet fires	Propane 230 Butane 255 203 to 287 crude oil	From the Barker LPG jet fire model. The SEPs are the capped values. From crude oil experiments.
Palacios et al. [60]	Jet fires	Mean 57.8 to 80.7	Results of large scale propane jet fire experiments.

Source	Applicable types of fire	Surface emissive power (kW m ⁻³)	Comments
Croce and Mudan [22]	Fireballs and jet fires	Methane 290 Ethane 360 Ethylene 500 Propane 340 n-butane 380 Propylene 280 Butylene 220	Based upon "Schmidt temperature measurements". Derived for jet fires but authors argue that they apply equally to fireballs.
Crawley et al. [67]	Fireballs and jet fires	Max 350	Taken from a series of tests by BP on oil fires and based on observed peak temperatures. Authors argue that actual SEP is likely to be nearer 275 kW m ⁻² . Methane flames are likely to have much lower SEPs.

Table 3 Summary of fraction of heat radiated, f , from the literature

Source	Type of fire	Fraction of heat radiated	Comments
Chamberlain [9]	Jet fires	$f = 0.21e^{-0.00323u_j} + 0.11$ $u_j = \text{jet velocity (m s}^{-1}\text{)}$	Based on wind tunnel tests and field trials.
Chaplin [8]	Jet fires	$f = 0.21e^{-0.00323u_j} + 0.11$ $u_j = \text{jet velocity (m s}^{-1}\text{)}$ $f = 0.38$ for two-phase jets	From Chamberlain [9]
Roberts [4]	Fireballs	$f = 0.27P^{0.32}$ up to $P = 6$ MPa $P = \text{the burst pressure (MPa)}$.	Based on small scale experiments of Hasegawa and Sato [12].

Source	Type of fire	Fraction of heat radiated	Comments
Prugh [23]	Fireballs	0.25 to 0.40	Inferred from flame temperatures.
Markstein [27]	Jet fires	0.2 to 0.25	For ethane and propane based on experimental data.
Cook et al. [36]	Jet fires	0.071 to 0.338	Field scale experiments of natural gas.
Cook et al. [37]	Jet fires	$f = 0.321 - 0.418 \times 10^{-3}u_j$ $u_j = \text{jet velocity (m s}^{-1}\text{)}$	Field scale experiments of natural gas.
Markstein [28]	Jet fires	0.17 to 0.3	
Cowley and Johnson [40]	Jet fires	0.2 for natural gas 0.3 for other hydrocarbons 0.2 for all fuels 0.25 for subsonic releases 0.1 for sonic releases	From the API point source model, based on small scale data. From the WHAZAN model. From the FLARESIM model.
Dutta et al. [41]	Jet fires	0.1 to 0.21	Crude oil with varying amounts of methane.
Johnson et al. [42]	Jet fires	$f = 0.21e^{-0.00323u_j} + 0.14$	Based on large scale natural gas experimental data.
Wade et al. [44]	Jet fires	0.1 to 0.45	Toluene mixed with hydrogen and methane
Lowesmith et al.	Jet fires	0.5 crude oil best fit value	Value reduces with increasing amounts

Source	Type of fire	Fraction of heat radiated	Comments
[51]		0.26 to 0.40 crude oil with 0% water 0.13 natural gas 0.24 propane 0.32 butane	of water in the crude. Largest crude oil release was 16 kg s ⁻¹ .
Cook et al. [56]	Jet fires	$f = \begin{cases} 0.21e^{-0.00323u_j} + 0.11 & MW < 21 \\ (0.21e^{-0.00323u_j} + 0.11) \left(\frac{MW}{21}\right)^{0.5} & 21 \leq MW \leq 60 \\ 1.69(0.21e^{-0.00323u_j} + 0.11) & MW > 60 \end{cases}$ u_j = jet velocity (m s ⁻¹) MW = molecular weight of the fuel (kg mol ⁻¹)	Based on Chamberlain [9] but with additional term to account for two-phase and liquid jets.
Kooi and Uijt de Haag [52]	Jet fires	0.12 to 0.47 0.35 to 0.67 for crude oil 0.15 to 0.45 for butane 0.1 to 0.39 butane/natural gas mixture 0.15 to 0.37 for propane 0.15 to 0.2	n-Butane modelled by the JFSH-Cook, Cracknell and Barker LPG jet fire models up to release rates of 10,000 kg s ⁻¹ . Experimental data. Release rates up to 30 kg s ⁻¹ . From Barnwell and Marshall [59]. Fraction of heat decreases with increasing exit velocity.
Croce and Mudan [22]	Fireballs and jet fires	For LNG 0.6 for gasoline	Origin unknown.

Source	Type of fire	Fraction of heat radiated	Comments
Lowesmith and Hankinson [69]	Fireballs and jet fires	0.25 to 0.4 for natural gas/hydrogen mixtures 0.2 to 0.3 for natural gas only	Large scale pipeline experiments.
Cleaver and Halford [70]	Fireballs and jet fires	$f = \min(0.5, \dot{m}_0^{-1/6})(0.28 + 0.31e^{-0.2U_{10}})$ \dot{m} = the mass flow rate (kg s ⁻¹) U_{10} = the wind speed at an elevation of 10 m (m s ⁻¹) Lower and upper limits are 0.07 and 0.35.	Equation is for the “stalk”. The “cap” is assumed to be 60% higher.

3.4.1 Fireballs

Currently within MISHAP, a value for the surface emissive power is assumed that depends on the amount of substance released. It does not vary according to the release substance. The values used are at the lower end of those observed in large scale experimental data (e.g. Roberts et al. [31]) for propane and butane fireballs. It is also lower than observed for releases of natural gas from high pressure pipelines (see Section 3.3.11).

Lower values of SEP counteract the cautious assumptions that the fireball is immediately at its maximum size and stays on the ground for its entire duration. For a revised fireball model where the fireball grows and rises, the current values of the SEP could be considered optimistic.

MISHAP does not vary the SEP according to the substance being modelled. The literature appears to indicate that the SEP can vary significantly, with lower values being observed for natural gas than for other hydrocarbons. As the soot content of the flame increases, the SEP increases. The soot content generally increases with increasing carbon content of the substance. It would therefore seem appropriate to adjust the SEP according to the substance modelled.

In contrast, there appears to be no justification for the change in SEP value that occurs in MISHAP when the fireball mass exceeds 125 te. There is very little information in the literature to indicate how the SEP will vary with size of fireball and the origins of the values used in MISHAP are unclear. From the literature it would appear reasonable to adjust the SEP with substance and not with fireball mass.

The SEP can be calculated, using the Stefan-Boltzmann equation, provided that the flame temperature and the flame emissivity are known. The temperature of the flame will depend on the substance. For model purposes, it can be assumed that the fire radiates as a black body, meaning that the flame emissivity can be assumed to be 1. In many cases, the flame temperature is not known. The fireball model for HSE either needs to calculate the flame temperature, which would need to be verified using available data, which is scarce, or an alternative method for calculating the SEP is required.

Flame temperatures for several substances have been quoted in Croce and Mudan [22], together with the corresponding SEPs. It could be possible to use these values, as an alternative to calculating the flame temperature in the fireball model. Experimental data (e.g. Johnson and Pritchard [21] and Roberts et al. [31]) has reported SEPs that are in reasonable agreement with those quoted by Croce and Mudan. The actual flame temperatures have not been reported in the experiments.

The experiments of Roberts et al. [31] indicate that the radiation increases rapidly over the first half of the fireball duration before decreasing to close to zero by extinction. This implies that the surface emissive power grows in the first stages of the fireball, reaches a maximum and then decreases again. This is similar to the theory presented by Martinsen

and Marx [29] where the SEP increases up to a maximum at 1/3 of the fireball duration and then decreases linearly for the remaining 2/3.

From the literature, Clay et al. [20] proposed a correlation for the SEP based on the burst pressure of the vessel, which appears to have been taken from Moorhouse and Pritchard [17]. It depends purely upon the pressure, with no account taken of the substance involved and was based on the small scale experiments of Hasegawa and Sato [12]. According to Moorhouse and Pritchard, it is only applicable for masses up to 6.2 kg, although it appears to have been applied to much larger releases as this restriction is not considered by Clay et al.

An alternative method is to calculate the SEP using the equation for a point source model, with the distance set to the fireball diameter (e.g. Martinsen and Marx [29]). This method requires knowledge of the fraction of the heat radiated, the mass of fuel involved, the heat of combustion, and the diameter and duration of the fireball (or the mass flow rate). The main issue with this method is around the estimation of the fraction of heat radiated. Alternatively, some authors have used the same equation but omitted the fraction of heat radiated. This is likely to lead to cautious values for the SEP.

From the literature, three correlations have been derived for the fraction of heat radiated. One of these is for jet fires (Chamberlain [9], with a modification by Cook et al. [36]) and the second is more general (Roberts [4]). The third has been derived for the initial stages of a natural gas pipeline rupture (Cleaver and Halford [70]). The correlation from Roberts uses the burst pressure and is based on the static vessel experiments of Hasegawa and Sato [12], whose experiments only considered fuel masses up to 6.2 kg and burst pressures of 1.35 MPa. Roberts extrapolated the correlation to burst pressures of up to 6 MPa, but acknowledged that there was a lack of data to validate this. This correlation has been used by a number of authors.

The Chamberlain correlation has been derived for natural gas jet fires and depends on the jet velocity. It is therefore not applicable to fireballs. The modification by Cook et al. includes the molecular weight, allowing it to be used for other substances. It is not clear what the basis for the modification is, however, given that the whole model has been validated against the natural gas experiments used by Chamberlain. The Cleaver and Halford correlation depends on the mass flow rate and the 10 m height wind speed and has been derived from predictions of another model.

The other method used in the wider literature to calculate the fraction of heat radiated requires knowledge of the SEP, making it unsuitable for the purposes of this report. Essentially, either the SEP or the fraction of heat is required, both of which have a considerable level of uncertainty associated with them.

More recent, large scale experiments have been performed for vessels (Johnson and Pritchard [21] and Roberts et al. [31]). It may be possible to derive a revised correlation for the fraction of heat radiated using the results from these experiments. It should be noted that the total number of experiments that could be considered as part of an analysis is 9,

limiting the applicability of any derived correlation. Given, however, that the existing correlation from Roberts [4] has been derived from a set of approximately 14 experiments, the largest of which consisted of a fuel mass of 6.2 kg, then it could be argued that a revised correlation will be just as applicable.

The second element of a solid flame model is the atmospheric transmissivity. The existing correlation used within MISHAP for the fireball model is believed to have been based on experimental data for pool fires using tables of data in Simpson [18] but no documentation has been found to substantiate this.

An alternative correlation is given by Clay et al. [20] but no information is given on its derivation or applicability.

Lihou and Maund [14] quote an equation that uses a visibility factor and the distance from the flame to the receiver. The origin of the equation is unclear, and Bagster and Pitblado [62] comment that the atmospheric transmissivity depends more on absorption than visibility.

The “Yellow Book” [25] contains an equation for transmissivity based on the partial water vapour pressure of water in air at any given relative humidity. This is a simplification based on relative humidity having little influence on the transmissivity provided that the transmissivity is expressed as a function of the partial water vapour pressure and the distance from the fireball to the receiver. The exact origin of the equation is unclear. Prugh [23] uses a slight variation on the equation in the “Yellow Book” but the origin is again uncertain.

A number of authors use the Wayne equations [30] to calculate atmospheric transmissivity. They are based on earlier work by Wyatt et al. [64], and Stull et al. [65] which was validated against experimental measurements of spectral transmissivity. The equations provide a simple way of considering the effects of both water and carbon dioxide on the absorption of the atmosphere. In addition, the atmospheric temperature and relative humidity are also considered. It is stated that the equations are suited to fires with a temperature of 1500 K but that the transmissivity does not vary greatly within a few hundred K of this value, making it applicable to a large number of fires.

3.4.2 Jet fires

As in the case of MISHAP, both the solid flame model and the point source, or multiple point source, methods have been used to calculate the radiation from a jet fire. The first of these methods requires knowledge of the SEP, or the flame temperature, and the second requires the fraction of heat radiated.

From the literature, there is some evidence that the temperature and hence the SEP varies along the length of a jet flame. This variation may need to be considered whether the solid flame model is used or a multiple point source model. For the solid flame model, either an average SEP could be used or the flame could be split into regions e.g. [60]. If a point source model is used, multiple points along the flame could be considered.

As in the case of fireballs, the issue with using the solid flame model is the uncertainty in the value of the SEP. In general, the values appear to lie between 200 and 350 kW m⁻², but there are a couple of references [54,60] that quote significantly lower values. An alternative method is to calculate the SEP from the flame temperature, but the temperature is often not known.

The point source model requires the fraction of heat radiated to be known or calculated. The values in the literature vary significantly. There are also a few correlations available but these have generally been derived from small-scale data and/or for a limited range of experimental conditions and substances. There is therefore considerable uncertainty over what values or equations should be used.

The fraction of heat radiated has been shown to be dependent on the fuel, the jet exit velocity and the discharge rate. A single value is therefore unlikely to represent the range of conditions that need to be modelled. Ideally an equation linking the fuel with the jet exit velocity and/or the discharge rate would be used. There is insufficient data, however, to derive such an equation.

4 Conclusions

The literature on radiation modelling with respect to fireballs and jet fires has been reviewed. It has been found that there are two main methods for modelling the radiation; the solid flame method and the point source method. The solid flame method is generally considered to be more accurate, particularly in the near field, but it can become complex as it takes the geometry of the flame into account.

The solid flame method requires the use of surface emissive power. The literature has shown considerable variation in the values of the surface emissive power, but it appears to vary by substance. The SEP can be calculated if the flame temperature is known, but this may not be the case for either the fireball or jet fire model. An alternative is to use the flame temperatures and calculated SEPs from Croce and Mudan [22]. These compare reasonably well against observed values.

In reality, the SEP will vary across the fire and will also vary during its duration. It could be possible, in the case of a fireball, to increase the SEP as the fireball grows and then decrease it to zero as the fireball dissipates. It is not clear, however, when the maximum value occurs and whether the SEP increases and decreases linearly or by some other method. Given all the uncertainties involved, it could be appropriate to use a single value throughout the duration of the fireball.

For jet fires, once a pseudo-steady state has been achieved, the assumption can be made that the SEP does not vary significantly. During its initial stages, however, the SEP could change and increase as the jet flame grows. As in the case of the fireballs, there is no data on which to base a varying SEP.

The solid flame model also requires the atmospheric transmissivity. From the literature, the most widely used method seems to be that of Wayne [30]. Other correlations have also been used but it is unclear how they have been derived.

The point source, or multiple point source model requires knowledge of the fraction of heat radiated. Several correlations have been suggested in the literature but they have limited applicability. A large number of values are also quoted but they show significant variation. It is clear, however, that the fraction of heat radiated is likely to be substance dependent. It has also been found to vary according to the jet exit velocity and the discharge rate.

In conclusion, when developing a new model a judgement will have to be made as to the most appropriate method and equations to use for calculating the radiation. This is due to the experimental data to validate any model being limited.

5 References

1. *Hazardous Substances*.
<http://planningguidance.communities.gov.uk/blog/guidance/hazardous-substances/>
(accessed July 2016).
2. *The Planning (Hazardous Substances) (Amendment) (England) Regulations 2009*.
<http://www.legislation.gov.uk/ukxi/2009/1901/body/made> (accessed November 2015).
3. *The Pipeline Safety Regulations (PSR) 1996*.
<http://www.legislation.gov.uk/ukxi/1996/825/contents/made> (accessed November 2015)
4. Roberts AF (1981). *Thermal radiation hazards from releases of LPG from pressurised storage*. Fire Safety Journal, Vol. 4, pp. 197-212, 1981/1982.
5. Chaplin Z (2022). *Fireball mathematical models and experimental data: A literature review*. HSE Research Report RR 1185,
<https://www.hse.gov.uk/research/rrhtm/rr1185.htm> (accessed February 2023).
6. Jackson A (2017). *Jet fire mathematical models for failure of pipelines carrying flammable substances: Part 1 Literature review*. HSE Research Report RR 1187,
<https://www.hse.gov.uk/research/rrhtm/rr1187.htm> (accessed March 2023).
7. Jackson A (2017). *Jet fire mathematical models for failure of pipelines carrying flammable substances: Part 2 Model Performance*. HSE Research Report RR 1188,
<https://www.hse.gov.uk/research/rrhtm/rr1188.htm> (accessed March 2023).
8. Chaplin Z (2015). *Rewriting MISHAP: The development of MISHAP12*. HSE Research Report RR 1040, <http://www.hse.gov.uk/research/rrhtm/rr1040.htm> (accessed January 2017).
9. Chamberlain GA (1987). *Developments in design methods for predicting thermal radiation from flares*. Chem. Eng. Res. Des., Vol. 65, pp. 299-309.
10. Fay JA, Desgroseilliers GJ and Lewis DH Jr (1979). *Radiation from burning hydrocarbon clouds*. Combustion Science and Technology, Vol. 20, pp. 141-151.
11. Fay JA and Lewis Jr DH (1977). *Unsteady burning of unconfined fuel vapour clouds*. Symposium (International) on Combustion, Vol. 16, Issue 1, pp 1397-1405.
12. Hasegawa K and Sato K (1977). *Study on the fireballs following steam explosion of n-pentane*. Proceedings of the second international symposium on loss prevention and safety promotion in the process industries, Heidelberg.
13. Williamson BR and Mann LRB (1981). *Thermal hazards from propane (LPG) fireballs*. Combustion Science and Technology, Vol. 25, pp. 141-145.

14. Lihou DA and Maund JK (1982). *Thermal radiation hazard from fireballs*. The Assessment of Major Hazards Symposium, IChemE Symposium Series No. 71, Manchester 14-16 April, 1982.
15. Stoll AM and Chianta MK (1971). *Heat transfer through fabrics as related to thermal injury*. Transactions of the New York Academy of Sciences, Vol. 33, Part 7, pp. 649-670.
16. Satyanarayana K, Borah M and Rao PG (1991). *Prediction of thermal hazards from fireballs*. J. Loss Prev. Process Ind., Vol. 4, pp. 344-347.
17. Moorhouse J and Pritchard MJ (1982). *Thermal radiation hazards from large pool fires and fireballs – a literature review*. IChemE North West Branch Symposium on the Assessment of Major Hazards, Manchester, April 1982.
18. Simpson IC (1984). *Atmospheric transmissivity – the effects of atmospheric attenuation on thermal radiation*. UKAEA, Safety and Reliability Directorate, SRD R304.
19. Partanen J and Vuorio M (1985). *Assessment of thermal radiation from LPG-fireballs*. Archivum Combustionis, Vol. 5, No. 2, pp. 127-143.
20. Clay GA, Fitzpatrick RD, Hurst NW, Carter DA and Crossthwaite PJ (1988). *Risk assessment for installations where liquefied petroleum gas (LPG) is stored in bulk vessels above ground*. Journal of Hazardous Materials, Vol. 20, pp. 357-374.
21. Johnson DM and Pritchard MJ (1991). *Large scale experimental study of boiling liquid expanding vapour explosions (BLEVEs)*. Gastech '90, 14th International LNG/LPG Conference & Exhibition, Gastech Ltd., Amsterdam, 4-7 December 1990.
22. Croce PA and Mudan KS (1986). *Calculating impacts for large open hydrocarbon fires*. Fire Safety Journal, Vol. 11, pp. 99-112.
23. Prugh RW (1994). *Quantitative evaluation of fireball hazards*. Process Safety Progress, Vol. 13, No. 2, pp. 83-91.
24. CCPS (1999). *Guidelines for chemical process quantitative risk analysis, 2nd Edition*. Center for Chemical Process Safety, American Institute of Chemical Engineers, New York.
25. TNO (2005). *Methods for the calculation of physical effects due to releases of hazardous materials (liquids and gases)*. *The Yellow Book*. TNO, The Netherlands.
26. Makhviladze GM, Roberts JP and Yakush SE (1999). *Fireball during combustion of hydrocarbon fuel releases. II. Thermal radiation*. Combustion, Explosion and Shock Waves, Vol. 35, No. 4, pp. 359-369.
27. Markstein GH (1976). *Radiative energy transfer from turbulent diffusion flames*. Combustion and Flame, Vol. 27, pp. 51-63.
28. Markstein GH (1988). *Correlations for smoke points and radiant emission of laminar hydrocarbon diffusion flames*. Twenty-second Symposium (International) on Combustion, The Combustion Institute, pp. 363-370.

29. Martinsen WE and Marx JD (1999). *An improved model for the prediction of radiant heat from fireballs*. International Conference and Workshop on Modeling Consequences of Accidental Releases of Hazardous Materials, San Francisco, California, September 28 – October 1, 1999.
30. Wayne FD (1991). *An economical formula for calculating atmospheric infrared transmissivities*. J. Loss Prev. Process Ind., Vol. 4, pp 86-92, January 1991.
31. Roberts T, Gosse A and Hawksworth S (2000). *Thermal radiation from fireballs on failure of liquefied petroleum gas storage vessels*. Trans IChemE, Vol. 78, Part B, pp. 184-192.
32. Novozhilov V (2003). *Some aspects of the mathematical modelling of fireballs*. Proceedings of the Institution of Mechanical Engineers, Vol. 217, Part E: J. Process Mechanical Engineering.
33. Abbasi T and Abbasi SA (2007). *The boiling liquid expanding vapour explosion (BLEVE): Mechanism, consequence assessment, management*. Journal of Hazardous Materials, Vol. 141, pp. 489-519.
34. CCPS (1999). *Guidelines for consequence analysis of chemical releases*. Center for Chemical Process Safety, American Institute of Chemical Engineers, New York.
35. Sonju OK and Hustad J (1984). *An experimental study of turbulent jet diffusion flames*. Presented at the 9th ICODERS, Poitiers, France, July 3- 8 1983.
36. Cook DK, Fairweather M, Hammonds J and Hughes DJ (1987). *Size and radiative characteristics of natural gas flares. Part 1 – Field scale experiments*. Chem. Eng. Res. Des., Vol. 65, pp. 310-317.
37. Cook DK, Fairweather M, Hammonds J and Hughes DJ (1987). *Size and radiative characteristics of natural gas flares. Part 2 – Empirical model*. Chem. Eng. Res. Des., Vol. 65, pp. 318-325.
38. Carter DA (1991). *Aspects of risk assessment for hazardous pipelines containing flammable substances*. J. Loss Prev. Process Ind., Vol. 4, pp. 68-72.
39. Shell Research (1991). *Large scale natural gas and LPG jet fires*. External report. TNER.91.022.
40. Cowley LT and Johnson AD (1992). *Oil and gas fires: Characteristics and impact*. Prepared by The Steel Construction Institute for the Health and Safety Executive, OTI 92 596, 1992.
41. Dutta P, Gore JP, Sivathanu YR and Sojka PE (1994). *Global properties of high liquid loading turbulent crude oil + methane/air spray flames*. Combustion and Flame. Vol. 97, pp. 251-260.
42. Johnson AD, Brightwell HM and Carsley AJ (1994). *A model for predicting the thermal radiation hazards from large-scale horizontally released natural gas jet fires*. IChemE Symposium Series No. 134, pp. 123-142.

43. Sekulin AJ and Acton MR (1995). *Large scale experiments to study horizontal jet fires of mixtures of natural gas and butane*. British Gas Research and Technology. GRC R 0367.
44. Wade R, Sivathanu YR and Gore JP (1995). *A study of two phase high liquid loading jet fires*. US Department of Commerce, National Institute of Standards and Technology, Report number NIS-GCR-95-678.
45. Selby CA and Burgan BA (1998). *Blast and fire engineering for topside structures: Phase 2*. The Steel Construction Institute.
46. Cumber PS (2000). *Ray effect mitigation in jet fire radiation modelling*. International Journal of Heat and Mass Transfer, Vol. 43, pp. 935-943.
47. Jo Y-D and Ahn BJ (2002). *Analysis of hazard areas associated with high-pressure natural-gas pipelines*. J. Loss Prev. Process Ind., Vol. 15, pp 179-188.
48. Cleaver RP, Cumber PS and Fairweather M (2003). *Predictions of free jet fires from high pressure, sonic releases*. Combustion and Flame, Vol. 132, pp. 463-474.
49. Lockwood FC and Shah NG (1981). *A new radiation solution method for incorporation in general combustion prediction procedures*. Eighteenth Symposium (International) on Combustion, Vol. 18, Issue 1, pp. 1405-1414.
50. Cumber PS (1995). *Improvements to the discrete transfer method of calculating radiative heat transfer*. J. Heat Mass Transfer, Vol. 38, pp. 2251-2258.
51. Lowesmith BJ, Hankinson G, Acton MR and Chamberlain G (2007). *An overview of the nature of hydrocarbon jet fire hazards in the oil and gas industry and a simplified approach to assessing the hazards*. Process Safety and Environmental Protection, Vol. 85, pp. 207-220.
52. Kooi ES and Uijt de Haag PAM (2012). *A comparison of jet fire models*. RIVM report 620550005/2012.
53. Gómez-Mares M, Muñoz M and Casal J (2009). *Axial temperature distribution in vertical jet fires*. Journal of Hazardous Materials, Vol. 172, pp. 54-60.
54. Gómez-Mares M, Muñoz M and Casal J (2010). *Radiant heat from propane jet fires*. Experimental Thermal and Fluid Science, Vol. 34, pp. 323-329.
55. Leroy G and Duplantier S (2010). *The 1D iterative model for predicting thermal radiation from a jet fire*. 6. International Seminar on Fire and Explosion Hazards (FEH), Leeds, UK.
56. Cook J, Bahrami Z and Whitehouse RJ (1990). *A comprehensive program for calculation of flame radiation levels*. Journal of Loss Prevention in the Process Industries, Vol. 3, pp. 150-155.
57. Kozanoglu B, Zárate L, Gómez-Mares M and Casal J (2011). *Convective heat transfer around vertical jet fires: An experimental study*. Journal of Hazardous Materials, Vol. 197, pp. 104-108.

58. Hankinson G and Lowesmith BJ (2012). *A consideration of methods of determining the radiative characteristics of jet fires*. Combustion and Flame, Vol. 159, pp. 1165-1177.
59. Barnwell J and Marshall BK (1985). *Offshore flare design to save weight*. AIChE annual meeting, 25 November 1984.
60. Palacios A, Muñoz M, Darbra RM and Casal J (2012). *Thermal radiation from vertical jet fires*. Fire Safety Journal, Vol. 51, pp. 93-101.
61. Crocker WP and Napier DH (1988). *Assessment of mathematical models for fire and explosion hazards of liquefied petroleum gases*. Journal of Hazardous Materials, Vol. 20, pp. 109-135.
62. Bagster DF and Pitblado RM (1989). *Thermal hazards in the process industry*. CEP, pp. 69-75.
63. Raj PPK (1977). *Calculations of thermal radiation hazards from LNG fires – a review of the state-of-the-art*. AGA Transmission Conference, 77-T-33, pp. T135-T148.
64. Wyatt PJ, Stull VR and Plass GN (1964). *The infrared transmittance of water vapour*. Applied Optics, Vol. 3, No. 2, pp. 229-241.
65. Stull VR, Wyatt PJ and Plass GN (1964). *The infrared transmittance of carbon dioxide*. Applied Optics, Vol. 3, No. 2, pp. 243-254.
66. Kay D (1994). *Thermal radiation heat transfer from flames to receiving targets*. AEA/CS/HSE R1006/R, HMSO Books, ISBN 0-853564045-1.
67. Crawley FK, Lines IG and Mather J (2003). *Oil and gas pipeline failure modelling*. Trans IChemE, Vol. 81, Part B, pp. 3-11.
68. Lehr WJ, Simecek-Beatty D and Muhasky J (2008). *Modeling fire and explosive risk in ALOHA*. Proceedings of the 31st AMOP Technical Seminar on Environmental Contamination and Response.
69. Lowesmith BJ and Hankinson G (2013). *Large scale experiments to study fires following the rupture of high pressure pipelines conveying natural gas and natural gas/hydrogen mixtures*. Process Safety and Environmental Protection, Vol. 91, pp. 101-111.
70. Cleaver RP and Halford AR (2015). *A model for the initial stages following the rupture of a natural gas transmission pipeline*. Process Safety and Environmental Protection, Vol. 95, pp. 202-214.
71. Acton MR, Baldwin PJ, Baldwin TR and Jager EER (1998). *The development of the PIPESAFE risk assessment package for gas transmission pipelines*. Proceedings of the International Pipeline Conference, Vol. 1, pp. 1-7.

The Health and Safety Executive (HSE) is a statutory consultee for planning applications around major hazard sites and pipelines and on applications for hazardous substances consent. HSE's advice is aimed at mitigating the effects of a major accident on the population around a major hazard site. This advice is informed by the use of mathematical models of potential hazards. HSE has an ongoing research programme to assess the suitability of the models used.

One of the potential hazards considered is a fireball or a jet fire that produces intense thermal radiation. A fireball occurs when there is immediate ignition of a pressurised release of flammable material in the event of a vessel or pipeline failure. A jet fire can occur underneath a fireball and remain after the fireball has dissipated, or if ignition is delayed.

This report describes a literature review of models that estimate the thermal radiation hazards, as well as experimental data that can be used to validate the models. The report details the different techniques available and any pipeline experimental data that was identified. The report includes identification of areas where there is a large variability in the parameters used in the modelling.

These findings are being used as part of the assessment of whether the fireball and jet fire models HSE currently uses are fit-for-purpose or whether changes would be beneficial.